



**AN ANALYTICAL EVALUATION OF THE SECOND
VIRIAL COEFFICIENT AND THE FIRST ORDER
QUANTUM CORRECTION TO THE SECOND VIRIAL
COEFFICIENT USING THE MORSE POTENTIAL**

HATUN ÇAÇAN

DOCTORATE THESIS

**DEPARTMENT OF PHYSICS
PROF. DR. BAHTİYAR MEHMETOĞLU**

APRIL - 2020

All rights reserved

**T.C.
TOKAT GAZIOSMANPASA UNIVERSITY
GRADUATE SCHOOL OF NATURAL & APPLIED SCIENCES
DEPARTMENT OF PHYSICS**

DOCTORATE THESIS

**AN ANALYTICAL EVALUATION OF THE SECOND VIRIAL COEFFICIENT AND
THE FIRST ORDER QUANTUM CORRECTION TO THE SECOND VIRIAL
COEFFICIENT USING THE MORSE POTENTIAL**

HATUN ÇAÇAN

**TOKAT
April- 2020**

All rights reserved

Hatun ÇAÇAN tarafından hazırlanan "An Analytical Evaluation of The Second Virial Coefficient and The First Order Quantum Correction to The Second Virial Coefficient Using The Morse Potential" adlı tez çalışmasının savunma sınavı 28 NİSAN 2020 tarihinde yapılmış olup aşağıda verilen Jüri tarafından Oy Birliği / Oy Çokluğu ile Tokat Gaziosmanpaşa Üniversitesi Fen Bilimleri Enstitüsü FİZİK ANA BİLİM DALI'nda DOKTORA TEZİ olarak kabul edilmiştir.

Jüri Üyeleri

İmza

Danışman
Prof. Dr. Bahtiyar MEHMETOĞLU



Üye
Prof. Dr. İbrahim YİĞİTOĞLU
Tokat Gaziosmanpaşa Üniversitesi



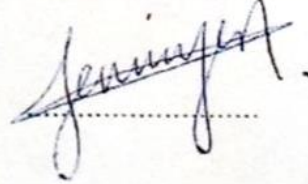
Üye
Prof. Dr. Ömer İŞILDAK
Tokat Gaziosmanpaşa Üniversitesi



Üye
Prof. Dr. Erhan ESER
Ankara Hacı Bayram Veli Üniversitesi



Üye
Doç. Dr. Selçuk DEMİREZEN
Amasya Üniversitesi



THESIS DECLARATION

I declare that the rules of scientific ethics are complied with in writing this doctoral thesis which is prepared in accordance with the thesis writing rules of Tokat Gaziosmanpasa University, Institute of Science and that it is referenced in accordance with the scientific norms in case of using the works of others, the novelty contained in the results and the results are not taken from any other reference and that no part of the thesis is presented as another thesis study at this university or another university.



Hatun ÇAÇAN

28th April, 2020

ABSTRACT

DOCTORATE THESIS

AN ANALYTICAL EVALUATION OF THE SECOND VIRIAL COEFFICIENT AND THE FIRST ORDER QUANTUM CORRECTION TO THE SECOND VIRIAL COEFFICIENT USING THE MORSE POTENTIAL

HATUN CACAN

TOKAT GAZIOSMANPASA UNIVERSITY
GRADUATE SCHOOL OF NATURAL AND APPLIED SCIENCES

DEPARTMENT OF PHYSICS

SUPERVISOR: PROF. DR. BAHTİYAR MEHMETOĞLU

The virial equation of state is valid over wide range of thermodynamic parameters and practical since it allows using intermolecular interaction potential models via virial coefficients to obtain thermodynamic properties accurately. For this purpose, an analytical formula for the second virial coefficient (SVC) with Morse potential is established and the obtained formula is applied to the SVC calculations of neutral atom gases and plasmas of *B, Si, Zn, H₂, N₂, O₂, NO, CO, He, Ne, Ar, Kr, Xe* and also for the speed of sound of *N₂, Ar* and *Zn* gases and found to provide reliable analytical solutions without any parameter restrictions. The first quantum correction to the SVC is also analytically evaluated with the Morse potential and applied for noble gases of *He, Ne, Ar, Kr, Xe* and also for *CH₄, CO₂, N₂* atoms and molecules for low temperatures. To our knowledge, except for some different approximation approaches, this study is the first analytical method for the calculation of the quantum correction to second virial coefficient with Morse potential and valid for all values of parameters. The SVC quantum correction results of Morse potential are compared with the literature especially with Lennard-Jones (12-6) and indicate a good agreement at higher temperatures of the investigated temperature range.

2020, 55 PAGES

KEYWORD: The Virial Equation of State, Second Virial Coefficient, Quantum Corrections, Morse Potential, Thermodynamic Properties.

ÖZET

DOKTORA TEZİ

İKİNCİ VİRİAL KATSAYISI VE İKİNCİ VİRİAL KATSAYISININ BİRİNCİ DERECE KUANTUM DÜZELTME İFADELERİNİN ANALİTİK OLARAK İNCELENMESİ

HATUN ÇAÇAN

TOKAT GAZİOSMANPAŞA ÜNİVERSİTESİ FEN BİLİMLERİ ENSTİTÜSÜ

FİZİK ANABİLİM DALI

TEZ DANIŞMANI: PROF. DR. BAHTİYAR MEHMETOĞLU

Termodinamik parametrelerin geniş aralıklarında geçerli olan virial hal denklemi virial katsayıları vasıtasıyla moleküller arası etkileşim potansiyeli modellerinin kullanımına olanak sağlamasıyla termodinamik özelliklerin elde edilmesinde kolaylık sağlar. Bu amaç doğrultusunda, Morse potansiyeli kullanılarak İkinci Virial Katsayısı (İVK) ifadesi için analitik bir formül elde edildi ve hiçbir parametre kısıtlaması olmadan güvenilir çözümler sunan bu analitik ifade $Si, Zn, H_2, N_2, O_2, NO, CO, He, Ne, Ar, Kr, Xe$ gaz ve plazmalarının nötral atomlarının İVK ve N_2, Ar and Zn gazlarının ses hızı hesaplamalarında kullanıldı. Düşük sıcaklıklarda ise İVK için birinci derece kuantum düzeltme ifadesi Morse potansiyeli kullanılarak analitik olarak hesaplandı ve soygazlardan He, Ne, Ar, Kr, Xe atomlarına ve ayrıca CH_4, CO_2, N_2 molekülleri için uygulandı. Bilindiği kadarıyla, bazı yaklaşık yöntemler dışında, bu çalışma İVK'nın quantum düzeltme hesaplamaları için Morse potansiyeli kullanılarak oluşturulan literatürdeki ilk analitik metottur ve parametrelerin tüm değerlerinde geçerli olduğu belirlenmiştir. Morse potansiyeli ile elde edilen İVK kuantum düzeltme ifadesi sonuçları literatürden Lennard- Jones (12-6) kullanılan sonuçlarla karşılaştırıldı ve araştırılan sıcaklık aralığının yüksek sıcaklıklarında uyum gözlemlendi.

2020, 55 SAYFA

ANAHTAR KELİMELELER: Virial Hal Denklemi, İkinci Virial Katsayısı, Kuantum Düzeltmeler, Morse Potansiyeli, Termodinamik Özellikler

ACKNOWLEDGEMENTS

I would like to express my special thanks to my advisor, Prof. Dr. Bahtiyar MEHMETOĞLU for supporting, encouraging and guiding me during my graduate study. His knowledge, experience, wisdom and patience guided me and made this research possible.

I am also deeply thankful to my husband Assoc. Prof. Dr. Ercan ÇAÇAN for his unconditional support that made me pursue my career. And my deepest thank goes to my kids Hazal Elif ÇAÇAN and Hilal Zehra ÇAÇAN, since they teach me the meaning of true love and increase my level of patience in life.

I owe a dept of gratitude to academic staff and research group members in Department of Physics at Tokat Gaziosmanpasa University and Giresun University, Prof. Dr. Birol ERTUĞRAL, Prof. Dr. İbrahim YİĞİTOĞLU, Assoc. Prof. M. Numan BAKIRCI, Dr. Ebru ÇOPUROĞLU, Dr. Elif SOMUNCU, Dr. Melek GÖKBULUT, Burcu UÇAR and Ebru KARATAŞ.

I'm eternally grateful for Dr. Sibel KARA and Dr. Mustafa Can KARA for their beautiful friendship that prevented all of us from being homesick in a foreign land. Finally, I would like to thank my loving and devoted mother, Emine ODABAŞI.

Hatun ÇAÇAN

April, 2020

CONTENTS

	<u>Page</u>
ABSTRACT	i
ÖZET	ii
ACKNOWLEDGEMENTS	iii
CONTENTS	iv
SYMBOLS AND ABBREVIATIONS	v
FIGURES LIST	vii
TABLES LIST	viii
1. INTRODUCTION	1
2. THEORETICAL FOUNDATIONS	7
2.1. Virial Equation of State	7
2.2. Classical Virial Coefficients	9
2.3. The Potential Effects on Second Virial Coefficient	13
2.4. Quantum Effects	16
2.5. Thermodynamic Properties	21
3. METODS AND RESULTS	24
3.1. A General Analytical Method for Evaluation of The Thermodynamic Properties of Matters Using Virial Coefficients with Morse Potential at High Temperature	24
3.1.1. Analytical expression of SVC with Morse potential	26
3.1.2. Computational results of the established formula and its application	31
3.2. The Comparative Analytical Evaluation of Quantum Corrections to The Second Virial Coefficient with Morse Potential and Its Applications to Real Systems	39
3.2.1. Analytical expressions of quantum correction to SVC with Morse potential	41
3.2.2. Computational results of quantum correction to the SVC and its applications on some atoms and molecules	44
4. CONCLUSION	47
5. REFERENCES	50
6. RESUME	55

SYMBOLS AND ABBREVIATIONS

Symbols	Explanation
α	Morse potential constant
b	Rydberg potential constant
$B(T)$	Temperature dependent second virial coefficient
γ	Adiabatic constant
c	Speed of sound
C_p	Constant pressure heat capacity
C_v	Constant volume heat capacity
$C(T)$	Temperature dependent third virial coefficient
ΔE	Internal energy change
ΔF	Gibbs free energy change
ΔH	Enthalpy change
ΔS	Entropy change
D and ε	Intermolecular potential well depth
$\bar{\varepsilon}$	Average energy of a particle
E_F	Fermi Energy
$f(r_{ij})$	Mayer function
h	Planck constant
H	Hamiltonian of the system
k_B	Boltzmann constant
Λ	Thermal de Broglie wavelength
Λ^*	Quantum mechanical parameter
λ	Absolute activity
m_e	Mass of electron
M	Molecular mass
n	Number density
\bar{n}_k	Average number of particles in the energy state k
N	Number of molecules inside the system

$\Xi(V, T, \mu)$	Grand partition function
P	Pressure
p	Momenta
$q(V, T)$	Molecular partition function
$Q(N, V, T)$	Classical canonical partition function
r	Intermolecular distance
r_e, r_0	Equilibrium intermolecular distance
ρ	Density
σ	Intermolecular distance when $U(r) = 0$
R	Universal gas constant
T	Temperature
$U(r)$	Intermolecular potential
V	Volume
z	Activity
Z	Compressibility
Z_N	Configuration integral
ψ_m	Wave function with a set of quantum numbers

Abbreviations

Explanation

DNA	Deoxyribonucleic acid
EoS	Equations of State
GCM	Generalized chemical model
ICF	Inertial confinement fusion
NASA	National Aeronautics and Space Administration
NIST	National Institute of Standards and Technology
RKR	Rydberg-Klein-Rees
SAXS	Small angle x-ray scattering
SIC	Self-interaction chromatography
SLS	Static light scattering
SVC	Second virial coefficient

FIGURES LIST

<u>Figure</u>	<u>Page</u>
Figure 2.1. a) Intermolecular potential curve. b) Mayer function $f(r_{12}) = e^{-U(r_{12})/k_B T} - 1$ versus intermolecular distance.....	11
Figure 2.2. The potential curve of O_2 for $^3\Sigma'$ state. Bold solid line RKR experimental potential, solid line Rydberg potential, dashed line Morse potential.....	14
Figure 2.3. Different potential models versus intermolecular distance r and their corresponding SVC values $B_2(T)$ versus temperature for argon. Holborn and Otto, Michels, Wijker, and Wijker graphs are based on the experimental SVC results	16
Figure 2.4. The Logn-LogT diagram of plasmas with terrestrial and cosmic examples	18
Figure 3.1. Dependence of the SVC with Morse potential (Eq. (3.2.9)) on temperature for He, Ne, Ar, Kr and Xe.....	38
Figure 3.2. Dependence of the SVC with Morse potential (Eq. (3.2.9)) on temperature for B, Si and Zn	38
Figure 3.3. Dependence of the SVC with Morse potential (Eq. (3.2.9)) on temperature for the molecules of H_2 , N_2 , O_2 , NO and CO.....	39

TABLES LIST

<u>Table</u>	<u>Page</u>
Table 3.1. Morse potential parameters for <i>Si, Zn, H₂, N₂, O₂, NO, CO, He, Ne, Ar, Kr, Xe</i>	32
Table 3.2 The comparative calculation results of SVC with Morse potential for the noble gases of <i>He, Ne, Ar, Kr</i> and <i>Xe</i> for different temperatures.....	33
Table 3.3 The comparative calculation results of SVC with Morse potential for semiconductors <i>B</i> and <i>Si</i> and a metal <i>Zn</i> for different temperatures.....	35
Table 3.4 The comparative calculation results of SVC with Morse potential for the molecules of <i>H₂, N₂, O₂, NO</i> and <i>CO</i> for different temperatures.....	36
Table 3.5 The speed of sound calculations for <i>Ar, N₂</i> and <i>Zn</i> by using the SVC results for the temperature range 3000- 7000 °K and pressures 0.1 and 1 atm.....	37
Table 3.6. Morse, Lennard- Jones and quantum mechanical parameters for <i>He, Ne, Ar, Kr, Xe, CH₄, CO₂</i> and <i>N₂</i>	45
Table 3.7. The comparative calculation results of quantum correction to SVC with Morse and Lennard-Jones (12-6) potentials for <i>He, Ne, Ar, Kr, Xe, CH₄, CO₂</i> and <i>N₂</i> for the temperature range of 40.9- 900 °K	46

1. INTRODUCTION

In the beginning of the 19th century, the heat was converted to mechanical energy by using the knowledge of energy conservation law known as the first law of thermodynamics. However, the effects of temperature on atoms and molecules in microscopic states had not been known yet. With the discovery of second law of thermodynamics, the irreversible processes of physical systems are explained by means of entropy. At the second half of 19th century, the fundamental principles of microscopic effects on macroscopic systems were able to be explained by probability and statistical mechanics by using entropy as a tool to connect microscopic and macroscopic systems (Logan, 1999).

The main purpose of natural sciences is the evaluation of physical, chemical and biological properties of matter in all aspects. It is well known that the matter in universe may exist in solid, liquid, gas, plasma or between any other possible transition states, which all require special equations of state (EoS) to evaluate its macroscopic properties. From these properties, evaluating matter in different states specifically for its thermodynamic properties is of importance by using probability and statistical mechanics (Olla, 2015).

A physical system can be described in various kinds of equations depending on its certain state associated with pressure, temperature and density at thermal equilibrium. The first equation of state is called ideal gas EoS, which is the beginning of thermodynamics and statistical mechanics of gases. When the pressure-temperature diagrams of matters are examined, it has been realized that applicability of ideal gas EoS is very limited and new EoS's are established creating new branches of physics.

The extreme states of matter (high pressure, temperature, density and velocity) have become the scientist's research interests with new theoretical and technical developments. Therefore, Maxwell-Boltzmann equation describing classical, non-relativistic and distinguishable particles has been incapable of explaining the relativistic and quantum effects dominated matter in the phase diagram. For this reason, different parts of the phase diagram of a substance have to be treated with different equations of state. For instance, the temperature increase in an ideal gas leads to ionization of gas (plasma), which EoS becomes Saha equation. Increasing temperature more results in non-degenerate gas with free electrons.

When we consider the pressure increase of the gas at which Fermi energy of the gas becomes much bigger than its thermal energy, the dominated quantum effects region with degenerate electron gas can be achieved, which EoS is changed to Fermi-Dirac EoS. When the degenerate electron gas at high pressure region ($P > 10^9$ atm) is considered, the Thomas-Fermi EoS is used. With the more increased pressure regions, completely degenerate and electron gases become relativistic except neutrons and protons. The highest pressure regions at very high densities allow reactions creating neutron stars (Eliezer et al., 2002).

The first correction to ideal gas EoS is van der Waals EoS taking into consideration of molecular interaction forces and molecular sizes. The Dieterici, Berthelot, Battie-Bridgeman, Peng-Robinson, Benedict-Webb-Rubin and Redlich-Kwong equations of state are also used for interactions of atoms and molecules, all of which have some limitations under some circumstances. Van der Waals, Dieterici and Berthelot equations of state have some difficulties during calculations of critical points. The Battie-Bridgeman EoS provides insufficient data for high pressure region of gaseous state (Beattie et. al., 1927; Beattie et. al, 1928; Hirschfelder et. al, 1954). The Benedict-Webb-Rubin EoS has limited temperature and density application region (Mamedov and Somuncu, 2014). The Redlich-Kwong EoS is applied only for the gaseous state but not appropriate for the liquids. The Peng-Robinson EoS was developed specifically for the liquid-vapor equilibrium properties of matter (Peng and Robinson, 1976).

In the region of interacting, neutral particles with a molecular size, using the virial equation of state is a reliable way for all temperature and pressure ranges of gases and neutral parts of partially ionized plasmas at generalized chemical model investigating low density plasmas. The virial EoS expansion includes additional terms in ideal gas EoS representing deviations arising from particle interactions. This virial EoS series expansion contains increasing number of virial coefficients starting from the second virial coefficient (SVC) demonstrating a volume with two interacting particles (McQuarrie, D. A., 1976). These increasing number of virial coefficients are used as a tool to reduce n-body problem of interacting particles to two body, three body and so on problems corresponding to the second, third and so on virial coefficients respectively depending on temperature, type of interaction potential and properties of gas under consideration. An analytical calculation of the virial coefficients becomes more complicated as the number of virial coefficient increases. Even for the SVC of simple hard sphere potential (constants being independent from temperature), second, third and fourth

virial coefficients can be calculated analytically while higher order virial coefficients (fifth to eleventh) need to be evaluated with numerical computation methods (Schultz and Kofke, 2014). These numerical methods include ab initio, Monte Carlo Simulation methods (Van, 2006), Molecular Dynamics, Density Functional Theory (Zeng, Ju and Xu, 2012) and Hartree-Fock (Aziz, 1993), Mayer sampling Monte Carlo technique (Ushcats, 2016) and semiclassical approximation (Hou, 2019). The computer simulation techniques allow evaluation of complex physical systems that analytical solutions are not currently possible or require approximations. The interaction potential value of the system has to be available as an input for the calculations in simulation systems (Van, 2006).

The SVC calculations are affected by the type of atoms and molecules some of which can not be described by summation of interacting particles' pair potentials. This nonadditivity issue arises from interatomic forces created by polarization and exchange effects (Kaplan, 2006). Some examples of this situation include atoms and molecules possessing electrical charge creating permanent dipole moments in molecules, which has to be considered by orientation and induction forces. The additive intermolecular interaction potentials include point like objects and rigid particles that do not depend on location of other particles such as intermolecular potential of spherical substances used for SVC calculations only depending on distance between the molecular centers of mass. However, the SVC of nonspherical atoms and molecules have to be evaluated considering induction, dispersion, electrostatic and shape effects. (Eslami et al., 2001). The most commonly used potentials for SVC of nonspherical substances are the Stockmayer, Keesom, dipolequadrupole, polarizable dipole, polarizable dipole-quadrupole, and polarizable dipole-quadrupole-steric (Johnson and Eubank, 1973). In addition, the SVC for polarizable molecules are also evaluated in literature (Haris and Alder, 1953).

Another nonadditivity issue arises from quantum mechanics since charges can not be described as rigid and point like particles. The quantum effects depending on the molecular weight together with temperature and density are also some of the influencing factors on the SVC calculations. Nearby and below the liquid transition region of low temperatures which classical virial expansion series diverges due to high density, therefore the quantum effects can not be ignored especially for lighter atoms such as H_2 , He and Ne . In this case of overwhelming quantum effects, scattering state wave functions and phase shifts of interaction potential have to be taken into account (McQuarrie, 1976). The quantum SVC calculations are

considered as a summation of SVC of quantum mechanical effects (B-direct) and exchange effects (B-exchange) evaluated by quantum statistics (Bruch, 1971). The exchange SVC formula is the reason for repulsion at short distances due to the asymptotic behavior of wave function of H_2 molecules with respect to permutations of electrons, which leads to phase-shifts (Boyd and Larsen, 1967). This repulsive exchange effects arising from the Pauli exclusion principle diminish rapidly with the distance. On the other hand, it is also possible to correct the classical SVC calculations nearby liquid-gas phase transition temperatures with another more practical formula called quantum correction, which is also calculated analytically for this study improving the accuracy of data especially for low temperatures.

A simple equation of state for the liquids do not provide enough accuracy, however when the accuracy is increased one has to deal with complex methods. Although virial equation of state diverges for the liquid substances, the SVC is used to create an analytical EoS for the liquids down to freezing temperatures with a sufficient accuracy (Song and Mason, 1990). This rather simple EoS includes three parameters: the SVC, scaling factor and the effective contact pair distribution function. Another EoS of the SVC for fluids is an acentric factor dependent linear equation (Pitzer and Curl, 1957). For the liquid mixtures, EoS of osmotic pressure in terms of the SVC is applied to biopolymers (Dewi et al., 2020). A more comprehensive study includes analytical calculations of the virial coefficients up to fourth virial coefficient for different D -dimensional fluids (Baus and Colot, 1987).

The current improvements in plasma physics researches dealing with laser interaction with matter, shock wave physics during especially inertial confinement fusions (ICF) and magnetic field applications on plasmas to create confinement in tokamaks require EoS to be evaluated and improved for these special cases. The SVC calculations are also important for fully ionized plasmas under the influence of constant magnetic field which is often encountered for the astrophysical aspects related to the physics of neutron stars and pulsars (Steinberg et al., 2000). The magnetic quantum SVC and EoS calculations for fully ionized plasmas are carried out in literature since their importance in application for the fields of quantum chaos as well as astrophysics (Hussein et al., 2012).

The SCV calculations also have another interesting and distinct application for determining the protein crystallization and solubility conditions and interactions between deoxyribonucleic acids (DNA). The static light scattering (SLS) and self-interaction chromatography (SIC) experimental methods are used to measure the value of osmotic SVC which should be

between -0.5×10^{-4} and -8.0×10^{-4} mol ml gr⁻² in order to form protein crystals in a solution. The SVC values lower than -0.5×10^{-4} mol ml gr⁻² indicate stronger attraction between proteins generating an amorphous solid and SVC values higher than -8.0×10^{-4} mol ml gr⁻² demonstrate a repulsive protein-protein interaction (Wilson, 2014). The small angle x-ray scattering (SAXS) method is applied to obtain the SVC values for DNA-DNA interactions (Li et al., 2008). The magnitude and sign of SVC indicates the strength and manner (repulsive or attractive) of the DNA-DNA interactions, respectively.

The value of temperature dependent second virial coefficient is also affected by the type of interaction potential. A very well-known and widely used two parameter Lennard-Jones (6-12) potential is a simple and practical choice for long range interactions (Galicia-Pimentel et al., 2006). However, the evaluation of high temperature phase diagram of substances requires a potential representing short range interactions well. The Morse and Rydberg potentials are good candidates for short range interactions and three parameter Morse potential is relatively easier to solve analytically. The Morse potential is suggested to be used for two body interactions of covalently bound diatomic molecules and metals (Lim, 2003), DNA denaturation (El Kinani et al., 2018), intermolecular interactions of cancer drugs (Naderi et al., 2009), liquid transport properties via molecular dynamics simulation (Galicia-Pimentel et al., 2006), crystal properties of cubic metals (Girifalco and Weizer, 1958), partially ionized plasmas (Apfelbaum, 2017). These diverse applications of the Morse potential in many research areas of literature make it a special potential to evaluate analytically, playing a key role to extend someone's research interest area beyond.

There are some experimental methods available in literature to determine the virial coefficients to validate analytical results. The experimental results of pressure, density and temperature are utilized to determine the second and third virial coefficients of a substance by using curve-fitting techniques or advanced graphical analysis (Cristancho et al., 2015). The compressibility factor obtained experimentally is another way of acquiring the SVC through the accurate interpolation of $P - V - T$ data (Deming and Shupe, 1931).

The recent progresses in plasma and astrophysics lead to investigation of thermodynamic properties at high temperature ranges as a recent topic. For this purpose, the Morse potential is chosen to evaluate high temperature low density neutral intermolecular interactions and thermodynamic properties of nonpolar substances. Using only SVC for low density gases to investigate the EoS and other thermodynamic properties and neutral interactions of partially

ionized plasmas is a good approximation. Therefore, an analytical solution for SVC with Morse potential is established and applied to real systems of $B, Si, Zn, H_2, N_2, O_2, NO, CO, He, Ne, Ar, Kr$ and Xe gases for this study. The results are compared with numerical calculations and another analytical formula from literature and found to have advantages over the literature when dealing with a substance having lower values of Morse parameters at high temperatures such as $Ar - He$ mixture plasmas (Pateyron, 1992). The obtained analytical formula of SVC with Morse potential is used for the calculation of speed of sound for Zn, Ar and N_2 gases at different temperature and pressure values and compared with literature (Mamedov and Cacan, 2019).

The evaluation of quantum corrections to SVC with Morse potential at low temperature region nearby the liquid transition of gases is also evaluated analytically for this study for $He, Ne, Ar, Kr, Xe, CH_4, CO_2$ and N_2 gases. The quantum correction effects onto the molecular weight and temperature is assessed comparatively (Cacan and Mamedov, 2019).

2. THEORETICAL FOUNDATIONS

2.1. Virial Equation of State

In order to derive virial EoS, we start with the grand partition function and derive pressure and density in term grand partition function (McQuarrie, 1976).

$$\Xi(V, T, \mu) = \sum_{N=0}^{\infty} Q(N, V, T) \lambda^N \quad (2.1.1)$$

where absolute activity is $\lambda = \exp(\mu/k_B T)$. In the case of $N = 0$, $Q(N = 0, V, T) = 1$.

$$\Xi(V, T, \mu) = 1 + \sum_{N=1}^{\infty} Q_N(V, T) \lambda^N \quad (2.1.2)$$

The relationship between the grand partition function and PV is given as:

$$PV = k_B T \ln \Xi \quad (2.1.3)$$

The average number of molecules in the system can be given as:

$$N = k_B T \left(\frac{\partial \ln \Xi}{\partial \mu} \right)_{V, T} = \lambda \left(\frac{\partial \ln \Xi}{\partial \lambda} \right)_{V, T} \quad (2.1.4)$$

A new activity z is assigned in terms of λ in such conditions that $z \rightarrow \rho$ as $\rho \rightarrow 0$. When $\lambda \rightarrow 0$, Eq.(2.1.4) becomes as following:

$$N = \lambda \left(\frac{\partial \ln \Xi}{\partial \lambda} \right)_{V, T} = \lambda Q_1 \quad (2.1.5)$$

As $\lambda \rightarrow 0$, then $\rho \rightarrow \lambda Q_1/V$. In these conditions z is appointed as $z = \lambda Q_1/V$. We designate a new parameter called configuration integral Z_N as:

$$Z_N = N! \left(\frac{V}{Q_1} \right)^N \quad (2.1.6)$$

The grand partition function can be given in terms of the new activity z as:

$$\Xi(V, T, \mu) = 1 + \sum_{N=1}^{\infty} \left(\frac{Q_N V^N}{Q_1^N} \right) z^N \quad (2.1.7)$$

A newly defined quantity Z_N can be used in Eq. (2.1.7).

$$\Xi = 1 + \sum_{N=1}^{\infty} \left(\frac{Z_N(V, T)}{N!} \right) z^N \quad (2.1.8)$$

The pressure can be written in powers of z as following:

$$P = k_B T \sum_{j=1}^{\infty} b_j z^j \quad (2.1.9)$$

We need to determine b_j in terms of Z_N . The Eqs (2.1.8) and (2.1.9) are substituted into $\Xi = \exp(PV/k_B T)$ and after some algebra.

$$b_1 = (1!V)^{-1} Z_1 = 1$$

$$b_2 = (2!V)^{-1} (Z_2 - Z_1^2)$$

$$b_3 = (3!V)^{-1} (Z_3 - 3Z_2 Z_1 + 2Z_1^3)$$

$$b_4 = (4!V)^{-1} (Z_4 - 4Z_3 Z_1 - 3Z_2^2 + 12Z_2 Z_1^2 - 6Z_1^4)$$

$$\dots \quad (2.1.10)$$

Now we have pressure in terms of activity z , we will have density in terms of z as well. Then, we will obtain pressure in terms of density.

$$\rho = \frac{N}{V} = \frac{\lambda}{V} \left(\frac{\partial \ln \Xi}{\partial \lambda} \right)_{V, T} = \frac{z}{V} \left(\frac{\partial \ln \Xi}{\partial z} \right)_{V, T} = \frac{z}{k_B T} \left(\frac{\partial P}{\partial z} \right)_{V, T} \quad (2.1.11)$$

Therefore, Eq.(2.1.12) can be obtained.

$$\rho = \sum_{j=1}^{\infty} j b_j z^j \quad (2.1.12)$$

We have both pressure and density in terms of z in Eqs.(2.1.9) and (2.1.12), respectively. The quantity z can be determined and eliminated by some algebra.

$$z = a_1\rho + a_2\rho^2 + a_3\rho^3 + \dots \quad (2.1.13)$$

Eq.(2.1.13) can be used in Eq. (2.1.12).

$$\begin{aligned} a_1 &= 1 \\ a_2 &= -2b_2 \\ a_3 &= -3b_3 + 8b_2^2 \\ &\dots \end{aligned} \quad (2.1.14)$$

When the obtained equations are substituted in Eq. (2.1.9), the virial equation of state as a power series expansion of number density (ρ) can be expressed as:

$$Z = \frac{P}{RT\rho} = 1 + B(T)\rho + C(T)\rho^2 + \dots \quad (2.1.15)$$

where Z is the compressibility factor, R is the universal gas constant, $B(T)$ and $C(T)$ are the temperature dependent second and third virial coefficients, respectively (Kaplan, 2006). The second and third virial coefficients can be given as:

$$B(T) = -b_2 = -(2!V)^{-1}(Z_2 - Z_1^2) \quad (2.1.16)$$

$$C(T) = 4b_2^2 - 2b_3 = -\frac{1}{3V^2}(V(Z_3 - 3Z_2Z_1 + 2Z_1^3) - 3(Z_2 - Z_1^2)^2) \quad (2.1.17)$$

Now, we can find Z_1 , Z_2 and Z_3 , then substitute the values into Eqs.(2.1.16) and (2.1.17).

2.2. Classical Virial Coefficients

In this section, the second and third virial coefficients will be derived and then, their physical significance will be discussed.

The classical canonical partition function of N atoms can be given as (McQuarrie, 1976):

$$Q = \frac{1}{N!h^{3N}} \int \dots \int e^{-H/k_B T} dp_1 \dots dp_N dr_1 \dots dr_N \quad (2.2.1)$$

where the Hamiltonian can be given as following:

$$H = \frac{1}{2m} \sum_{n=1}^{\infty} p_{x_n}^2 + p_{y_n}^2 + p_{z_n}^2 + U(x_1, y_1, \dots, z_N) \quad (2.2.2)$$

As a result of integration over momenta for Eq.(2.2.1), the partition function is obtained as:

$$Q = \frac{1}{N!} \left(\frac{2\pi m k_B T}{h^2} \right)^{3N/2} Z_N \quad (2.2.3)$$

The configuration integral Z_N is defined as:

$$Z_N = \int \int e^{-U_N/k_B T} d\mathbf{r}_1 d\mathbf{r}_2 \dots d\mathbf{r}_N \quad (2.2.4)$$

For the conditions of $N = 1$ and $U = 0$ (no external force), Eq. (2.2.3) becomes:

$$Q_1 = \left(\frac{2\pi m k_B T}{h^2} \right)^{3/2} V = \frac{V}{\Lambda^3} \quad (2.2.5)$$

where Λ is the thermal de Broglie wavelength. Eq.(2.2.1) can be integrated over the momenta for $N > 1$.

$$Q_N = \frac{1}{N!} \left(\frac{Q_1}{V} \right)^N Z_N \quad (2.2.6)$$

Now we can derive the first three configuration integrals of Z_1, Z_2 and Z_3 appearing in Eqs.(2.1.15) and (2.1.16) to determine $B(T)$ and $C(T)$.

$$Z_1 = \int d\mathbf{r}_1 = V \quad (2.2.7)$$

$$Z_2 = \int \int e^{-U_2/k_B T} d\mathbf{r}_1 d\mathbf{r}_2 \quad (2.2.8)$$

$$Z_3 = \int \int \int e^{-U_3/k_B T} d\mathbf{r}_1 d\mathbf{r}_2 d\mathbf{r}_3 \quad (2.2.9)$$

In order to determine the SVC, intermolecular potential $U_2(r_1, r_2)$ is considered to depend only on the distance between two monoatomic particles as $U_2 = u(r_{12})$, where $r_{12} = |r_2 - r_1|$. After substituting Eqs.(2.2.7) and (2.2.8) into Eq.(2.1.16), The SVC can be obtained as:

$$B(T) = -\frac{1}{2V} (Z_2 - Z_1^2) = -\frac{1}{2V} \int \int \left[e^{-u(r_{12})/k_B T} - 1 \right] d\mathbf{r}_1 d\mathbf{r}_2 \quad (2.2.10)$$

Since the coordinate elements $d\mathbf{r}_1$ and $d\mathbf{r}_2$ are close to each other, it is possible to change integration variables.

$$B(T) = -\frac{1}{2V} \int d\mathbf{r}_1 \int [e^{-u(r_{12})/k_B T} - 1] d\mathbf{r}_{12} \quad (2.2.11)$$

When the values of $d\mathbf{r}_1 = V$ and $d\mathbf{r}_{12} = 4\pi r^2$ are substituted into Eq.(2.2.11), the SVC becomes:

$$B(T) = -2\pi \int_0^{\infty} [e^{-U(r)/k_B T} - 1] r^2 dr \quad (2.2.12)$$

where $f(r_{ij}) = e^{-U(r_{ij})/k_B T} - 1$ is called the Mayer function and $r_{ij} = r_{12}$ for the SVC calculations, which represent the interaction of two particles. The Eq.(2.2.12) can be integrated by parts to express the SVC in a different way (Vargas et al., 2000).

$$B(T) = -\frac{2\pi}{3k_B T} \int_0^{\infty} \frac{dU(r)}{dr} e^{-U(r)/k_B T} r^3 dr \quad (2.2.13)$$

According to Eq. (2.2.12), the SVC is independent from the diatomic interaction volume and shape of the potential curve but it depends on temperature and the integral representing the area limited by potential curve (Monajjemi et al., 2012). A typical potential curve and a graph of Mayer function for the SVC is represented in Figure 2.1 (McQuarrie, 1976)

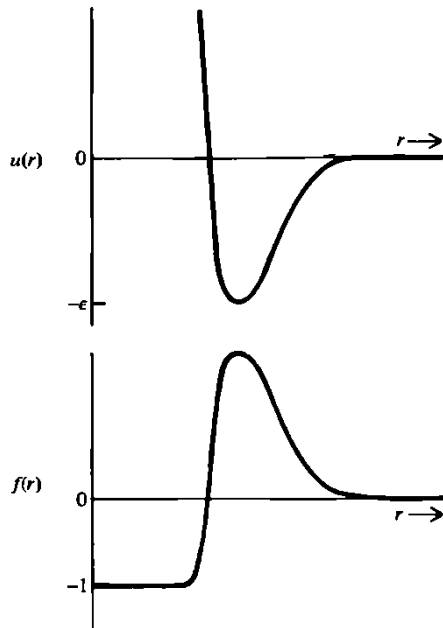


Figure 2.1. a) Intermolecular potential curve. b) Mayer function $f(r_{12}) = e^{-U(r_{12})/k_B T} - 1$ versus intermolecular distance (McQuarrie, 1976).

In order to derive the third virial coefficient, the intermolecular potential $U_3(\mathbf{r}_1, \mathbf{r}_2, \mathbf{r}_3)$ has to be determined by using pairwise additivity of intermolecular forces and deviations from pairwise additivity represented by Δ .

$$U_3 = u(r_{12}) + u(r_{13}) + u(r_{23}) + \Delta(r_{12}, r_{13}, r_{23}) \quad (2.2.14)$$

The pairwise additivity deviations will be neglected for the following derivations. To derive $C(T)$, Eq.(2.1.17) shows that b_3 has to be determined which is given by $6Vb_3 = Z_3 - 3Z_2Z_1 + 2Z_1^3$. The Z_3 is given as:

$$\begin{aligned} Z_3 &= \iiint (1 + f_{12})(1 + f_{13})(1 + f_{23}) d\mathbf{r}_1 d\mathbf{r}_2 d\mathbf{r}_3 \\ &= \iiint (f_{12}f_{13}f_{23} + f_{12}f_{13} + f_{12}f_{23} + f_{13}f_{23} + f_{12} + f_{13} + f_{23} + 1) d\mathbf{r}_1 d\mathbf{r}_2 d\mathbf{r}_3 \end{aligned} \quad (2.2.15)$$

The value of Z_2Z_1 can be given with three equivalent equations, therefore each one will be taken into consideration to create $-3Z_2Z_1$, where $Z_1 = V$.

$$\begin{aligned} Z_1Z_2 &= V \iint (f_{12} + 1) d\mathbf{r}_1 d\mathbf{r}_2 = \iiint (f_{12} + 1) d\mathbf{r}_1 d\mathbf{r}_2 d\mathbf{r}_3 \\ &= V \iint (f_{13} + 1) d\mathbf{r}_1 d\mathbf{r}_3 = \iiint (f_{13} + 1) d\mathbf{r}_1 d\mathbf{r}_2 d\mathbf{r}_3 \\ &= V \iint (f_{23} + 1) d\mathbf{r}_2 d\mathbf{r}_3 = \iiint (f_{23} + 1) d\mathbf{r}_1 d\mathbf{r}_2 d\mathbf{r}_3 \end{aligned} \quad (2.2.16)$$

Therefore the value of $Z_3 - 3Z_2Z_1$ becomes:

$$Z_3 - 3Z_1Z_2 = \iiint (f_{12}f_{13}f_{23} + f_{12}f_{13} + f_{12}f_{23} + f_{13}f_{23} - 2) d\mathbf{r}_1 d\mathbf{r}_2 d\mathbf{r}_3 \quad (2.2.17)$$

The last term to get $6Vb_3$ is $2Z_1^3 = 2 \iiint d\mathbf{r}_1 d\mathbf{r}_2 d\mathbf{r}_3$.

$$6Vb_3 = \iiint (f_{12}f_{13}f_{23} + f_{12}f_{13} + f_{12}f_{23} + f_{13}f_{23}) d\mathbf{r}_1 d\mathbf{r}_2 d\mathbf{r}_3 \quad (2.2.18)$$

In Eq.(2.1.17), $C(T)$ is given as $4b_2^2 - 2b_3$. The value of $C(T)$ can be rearranged to include $6Vb_3$ as:

$$C(T) = -\frac{1}{3V}(6Vb_3 - 12Vb_2^2) \quad (2.2.19)$$

The last term to determine $C(T)$ is $12Vb_2^2$, which can be obtained as:

$$4b_2^2 = \left[\int f_{12} d\mathbf{r}_{12} \right]^2 = \left[\int f_{12} d\mathbf{r}_{12} \right] \left[\int f_{13} d\mathbf{r}_{13} \right] \quad (2.2.20)$$

$$4Vb_2^2 = \int d\mathbf{r}_1 \int f_{12} d\mathbf{r}_{12} \int f_{13} d\mathbf{r}_{13} = \iiint f_{12} f_{13} d\mathbf{r}_1 d\mathbf{r}_2 d\mathbf{r}_3$$

Two more equivalent equations to Eq.(2.2.20) can be derived by using $f_{13}f_{23}$ and $f_{12}f_{23}$. Therefore, these three equations together form the $12Vb_2^2$ to be subtracted from $6Vb_3$. Finally, the third virial coefficient can be obtained.

$$C(T) = -\frac{1}{3V} \iiint f_{12} f_{13} f_{23} d\mathbf{r}_1 d\mathbf{r}_2 d\mathbf{r}_3 \quad (2.2.21)$$

The Eq.(2.2.21) represents interaction of three particles which are close to each other enough to interact since the related Mayer functions vanish for large separations between pair of particles.

2.3. The Potential Effects on Second Virial Coefficient

The intermolecular interactions between atoms and molecules of a system form a curve displaying potential energy versus intermolecular distance of the system. This curve contains important information such as potential well depth, equilibrium distance, force and anharmonicity constants. In order to provide reliable information for the interactions, a potential curve should satisfy some necessary conditions (Varshni, 1957). When the intermolecular distance $r = 0$, the value of potential should be $U = \infty$ or large enough representing very large repulsive force due to atomic or molecular volume. At $r = r_e$, potential should have a minimum where attractive and repulsive forces are in equilibrium. When $r \rightarrow \infty$, the attractive forces become dominant and potential has to reach a constant value asymptotically.

In order to have a good representation of interactions, a widely used two parameter Lennard-Jones (6-12) potential is suggested to obtain virial coefficients and thermodynamic properties of non-bonded noble gas atoms. Since the Lennard Jones (6-12) potential is inadequate to describe more interacting gases and molecules, it is modified to be used for metals as Lennard- Jones (n-m) including adjustable potential parameters specifically determined for the metals under consideration (Zhen and Davies, 1983). Another potential similar to Lennard- Jones (6-12) but theoretically more accurate is called the Buckingham (exp-6)

potential which is also modified due to its incorrect approach for small intermolecular distances (for $r = 0, U(r) = -\infty$).

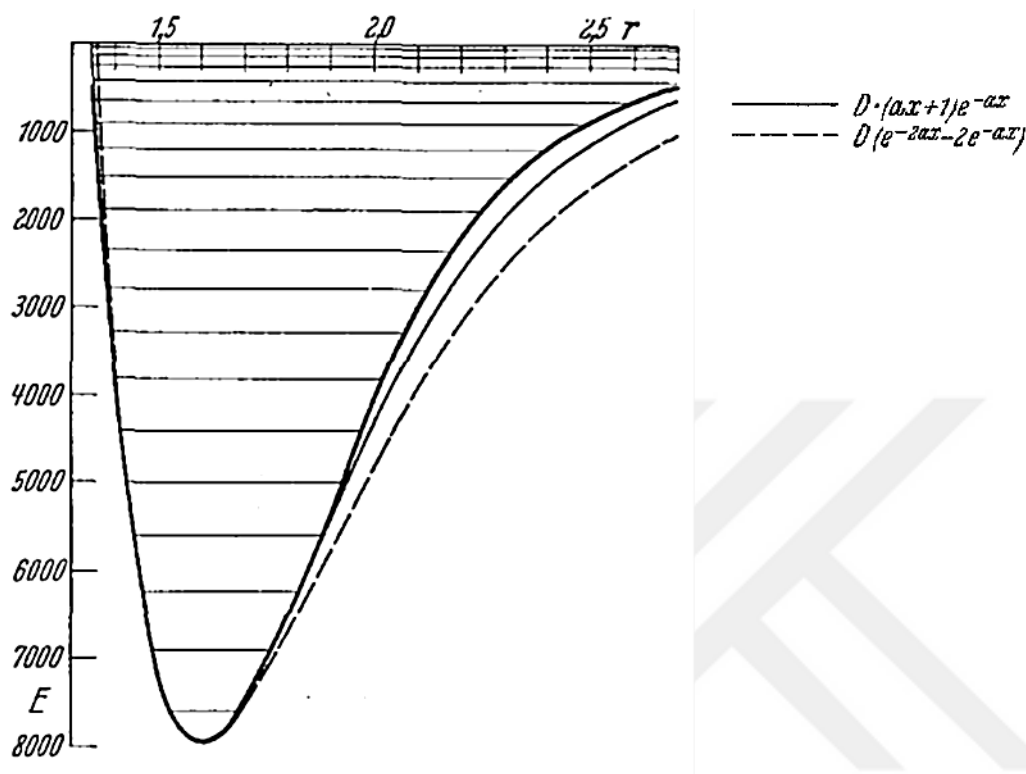


Figure 2.2. The potential curve of O_2 for $^3\Sigma'$ state. Bold solid line RKR experimental potential, solid line Rydberg potential, dashed line Morse potential (Rydberg, 1931).

A theoretically successful choice of potential for the calculation of SVC can be determined by using experimental data. For this purpose, Rydberg–Klein–Rees (RKR) method allows the reconstruction of the potential curve by using experimental spectroscopic data. Therefore, the RKR model is utilized for the comparative analysis between model potentials to determine the mean deviation from the RKR experimental potential curve. The percent errors of potentials are reported as 3.68 % for the Morse, 3.48% for the Pöschl-Teller and 2.94% for the Rydberg potential (Kaplan, 2006).

The evaluation of SVC by using various potentials is available in literature such as Lennard-Jones (6-12), Rydberg, Morse, Keesom, Stockmayer and Boys- Shavitt potentials (Kaplan, 2006). The correct choice of potential depends on temperature range of study and structure of the substance under evaluation as it is stated at introduction. Figure 2.3.1 displays the

potential curves of Rydberg, Morse and RKR experimental potentials of O_2 for $^3\Sigma'$ state. The Rydberg potential demonstrates a better curve being more close to the experimental RKR curve since Morse potential includes an exponential attraction term leading to over estimation of attractive forces for long ranges. Since long range attractive forces are negligible at high temperatures, Morse potential can be a good candidate for representation of dominant strong short range repulsion forces with its exponential repulsion term. The Morse, Rydberg, Lennard- Jones (6-12) and Lennard- Jones (m-n) potential formulae are provided in Eqs(2.3.1)-(2.3.4), respectively.

$$U(r)_M = D\{exp[-2\alpha(r - r_e)] - 2exp[-\alpha(r - r_e)]\}. \quad (2.3.1)$$

$$U(r)_R = D[1 + b(r_{ij} - r_0)]e^{-b(r_{ij}-r_0)} \quad (2.3.2)$$

$$U(r)_{L-J(6-12)} = 4\epsilon \left\{ \left(\frac{\sigma}{r} \right)^{12} - \left(\frac{\sigma}{r} \right)^6 \right\} \quad (2.3.3)$$

$$U(r)_{L-J(m-n)} = \epsilon \left\{ \frac{m}{n-m} \left(\frac{r_0}{r} \right)^n - \frac{n}{n-m} \left(\frac{r_0}{r} \right)^m \right\} \quad (2.3.4)$$

where potential parameters D and ϵ are in energy units, σ , r_e and r_0 are in length units and b and α are in reciprocal of length units.

In Figure 2.3, $B(T) = 0$ at a special temperature called as Boyle's temperature (T_B) at which gas molecules behave ideally since attractive and repulsive forces become equal. In literature, T_B value of Argon is reported to be 410,151 °K for the Lennard- Jones (6-12) potential (Somuncu, 2018).

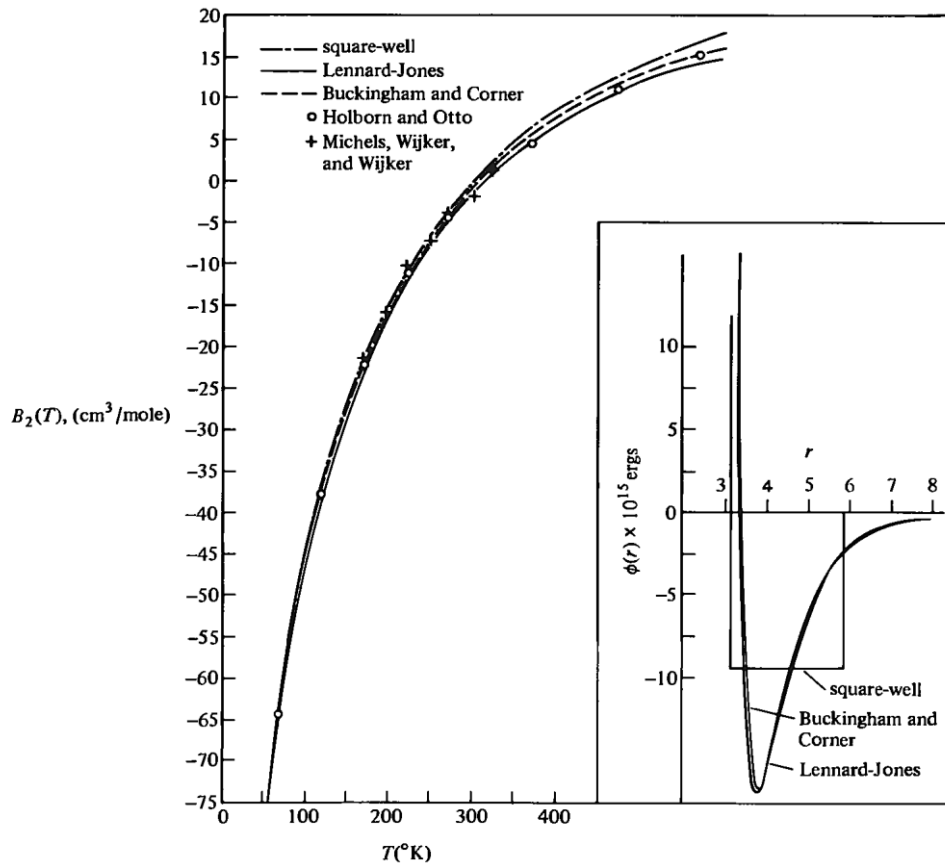


Figure 2.3. Different potential models versus intermolecular distance r and their corresponding SVC values $B_2(T)$ versus temperature for argon. Holborn and Otto, Michels, Wijker, and Wijker graphs are based on the experimental SVC results (McQuarrie, 1973).

2. 4. Quantum Effects

In quantum mechanics, in order uncertainty principle to be applicable, d separation between particles has to be in order of de Broglie wavelength being proportional to uncertainty in position Δx , so that particles wavelengths overlap ($\Delta x \approx \frac{\hbar}{2} \approx \lambda_B$ and $\Delta x \approx d$ or $\lambda_B \approx d$). Therefore, the quantum physics is applicable if the value of de Broglie wavelength λ_B is close or higher than the average distance between particles which is proportional to number density as $d \sim n^{-1/3}$. This case can be expressed as $n\lambda_B^3 \geq 1$ and valid for high number density n or low temperature of gases under consideration. According to equipartition theorem, average energy of every particle in a gas with momentum P and temperature T is $\frac{P^2}{2m} = \frac{3}{2}k_B T$. We can substitute the value of momentum in de Broglie wavelength as $\lambda_B = \frac{h}{\sqrt{3mk_B T}}$. Therefore, number density and temperature values play the key role to determine the behavior of gases

and plasmas and the gasses with smaller molecular mass m encounter more quantum effects at the same temperature (Karaođlu, 2009).

In quantum statistics, two main statistical distribution laws representing the identical particles with half integer spins and integer values of spins called Fermi-Drac and Bose-Einstein statistics, respectively. The main equations associated with these laws are represented by (+) sign for the Fermi-Drac statistics and (-) sign for the Bose-Einstein statistics in Eqs.(2.4.1) (McQuarrie, 1976).

$$\begin{aligned}
 \Xi(V, T, \lambda) &= \prod_k (1 \pm \lambda e^{-\beta \varepsilon_k})^{\pm 1} \\
 \bar{n}_k &= \frac{\lambda e^{-\beta \varepsilon_k}}{1 \pm \lambda e^{-\beta \varepsilon_k}} \\
 N &= \sum_k \bar{n}_k = \sum_k \frac{\lambda e^{-\beta \varepsilon_k}}{1 \pm \lambda e^{-\beta \varepsilon_k}} \\
 E &= N \bar{\varepsilon} = \sum_k \bar{n}_k \varepsilon_k = \sum_k \frac{\lambda \varepsilon_k e^{-\beta \varepsilon_k}}{1 \pm \lambda e^{-\beta \varepsilon_k}} \\
 PV &= \pm k_B T \sum_k \ln(1 \pm \lambda e^{-\beta \varepsilon_k})
 \end{aligned} \tag{2.4.1}$$

where N is the number of particles, \bar{n}_k is the average number of particles in the energy state of k and $\bar{\varepsilon}$ is the average energy of a particle. The analytical solutions of Eqs.(2.4.1) is not available when $\lambda \rightarrow 0$ indicating the reduction of Eqs.(2.4.1) to the classical Boltzmann statistics that require $\lambda = \frac{N}{q}$ where q is the molecular partition function. For this reason, the value of λ is the indicator of behavior of a system whether it is a quantum or classical statistics. The value of λ is small when the density of a system is low and its temperature is high corresponding to a classical Boltzmann statistics. However, the quantum statistical behavior is expected for a system when λ is large which is the case for high density and low temperature values of a system (McQuarrie, 1973). Therefore, number density and temperature values play the key role to determine the behavior of gases and plasmas.

$n - T$ diagram of gases and plasmas can be divided into some areas in order to be treated by an appropriate physical method. These areas are determined by the non-ideality and degeneracy parameters. A plasma is considered as ideal if the ratio of the particle's electrical interaction energy over thermal energy is lower than 1 ($\Gamma = \frac{e^2 n^{1/3}}{\varepsilon_0 k_B T} < 1$). If the particle's ratio

of thermal energy over Fermi energy is much higher than 1, the plasma becomes classical (non-degenerate) ($\theta = \frac{k_B T}{E_F} = \frac{2mk_B T}{\hbar^2} (3\pi^2 n_e)^{-2/3} \gg 1$). The quantum effects are dominant if the degeneracy parameter becomes lower than 1 which is only possible with high number density or low temperature values. Another parameter r_s is defined as quantum criteria of ideality and it represents the ratio of electrical interaction energy to Fermi energy. The condition of $r_s < 1$ represents the ideal quantum gas region. Figure 2.4 illustrates the $n - T$ diagram with non-ideality and degeneracy parameters (Omarbakiyeva, 2010).

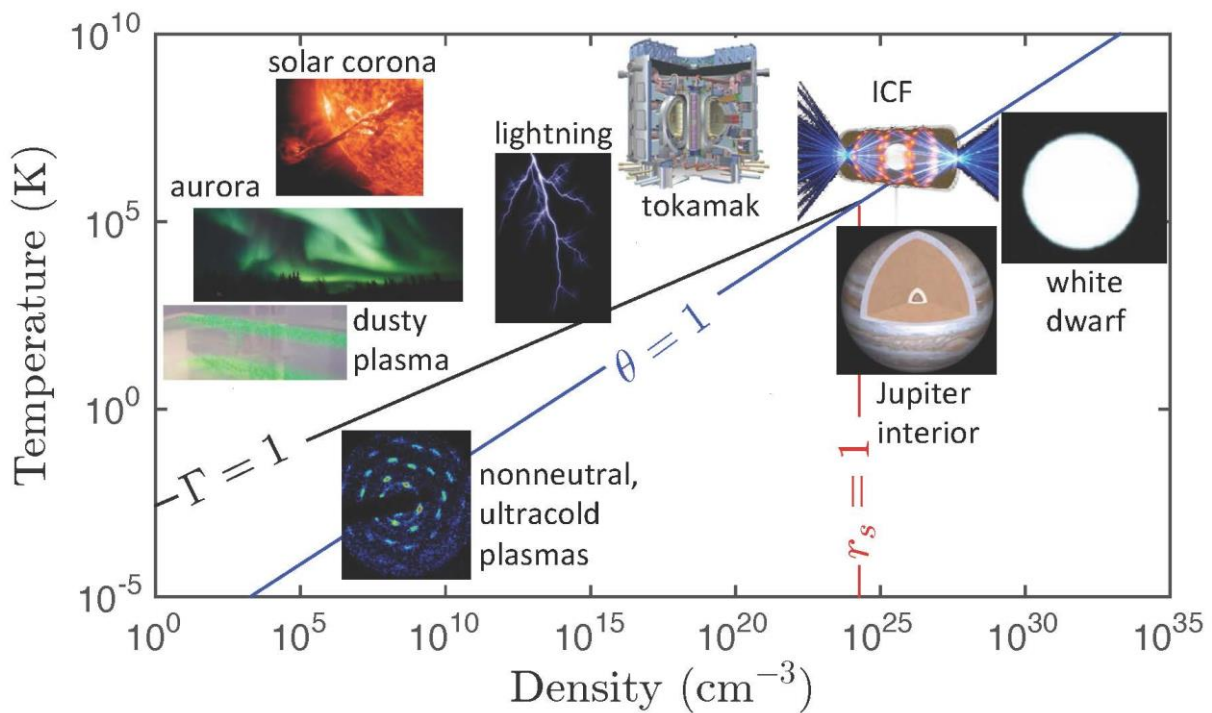


Figure 2.4. The $\text{Log}n - \text{Log}T$ diagram of plasmas with terrestrial and cosmic examples (Omarbakiyeva, 2010).

In this research, an analytical evaluation of the SVC with Morse potential is carried out for high temperature region which is also suitable for the structure of Morse potential. Therefore, dominant quantum effects for low temperature region are avoided. However, an analytical evaluation of the quantum correction with Morse potential is obtained nearby liquid transition region of some atoms and molecules at low temperature region.

The expression of the first quantum correction arises from statistical thermodynamics. The translational and rotational degrees of freedom of interacting molecules can be considered classical since separations between levels are so small to be treated by an integral. However, vibrational degrees of freedom have to be discussed quantum mechanically. Therefore, the Hamiltonian of a system of interacting molecules and partition function become (McQuarrie, 1973).

$$H = H_{class} + H_{quant}$$

$$Q = Q_{class} Q_{quant} \quad (2.4.2)$$

where classical canonical partition function can be defined as:

$$Q_{class} = \frac{1}{N! h^{3N}} \int e^{-H_{class}(\mathbf{p}, \mathbf{q})/k_B T} d\mathbf{p}_{class} d\mathbf{q}_{class}. \quad (2.4.3)$$

The quantum mechanical form of the canonical partition function represented by the summation of energy states can be reduced to classical one when $\hbar \rightarrow 0$.

$$Q = \sum_j e^{-E_j/k_B T} \xrightarrow{\hbar \rightarrow 0} \frac{1}{N! h^{3N}} \int \dots \int e^{-H/k_B T} d\mathbf{p}_1 \dots d\mathbf{p}_N d\mathbf{q}_1 \dots d\mathbf{q}_N \quad (2.4.4)$$

Now, we need an expression for the canonical partition function including non-ideal systems. A general expression for the quantum correction can be derived starting from the partition function.

$$Q_N = \sum_m \int \psi_m^* e^{-\beta H} \psi_m d\mathbf{r}_1 \dots d\mathbf{r}_N \quad (2.4.5)$$

where $\beta = 1/k_B T$.

The canonical partition function can be expressed as a power series of \hbar , the first term being the classical partition function without the $N!$ due to neglected symmetry of the wave functions (Kirkwood, 1933).

$$Q_N = \frac{1}{h^{3N}} \int \dots \int e^{-\beta H} w(\mathbf{p}_1 \dots \mathbf{r}_N, \beta) d\mathbf{p}_1 \dots d\mathbf{r}_N \quad (2.4.6)$$

where the function $w(\mathbf{p}_1, \dots, \mathbf{r}_N, \beta)$ is the representation of the quantum correction to the classical partition function. This function is simply reduced to 1 as $\hbar \rightarrow 0$ or $\beta = 0$ and given as:

$$w(\mathbf{p}_1, \dots, \mathbf{r}_N, \beta) = \sum_{l=0}^{\infty} \hbar^l w_l(\mathbf{p}_1, \dots, \mathbf{r}_N, \beta). \quad (2.4.7)$$

When the Eq.(2.4.7) is expanded, the first three expressions can be obtained as:

$$\begin{aligned} w_0 &= 1 \\ w_1 &= -\frac{i\beta^2}{2m} \sum_{j=1}^N \mathbf{p}_j \cdot \nabla_j U \\ w_2 &= -\frac{1}{2m} \left\{ \frac{\beta^2}{2} \sum_{k=1}^N \nabla_k^2 U - \frac{\beta^3}{3} \left[\sum_{k=1}^N (\nabla_k U)^2 + \frac{1}{m} \left(\sum_{k=1}^N \mathbf{p}_k \cdot \nabla_k \right)^2 U \right] + \frac{\beta^4}{4m} \left(\sum_{k=1}^N \mathbf{p}_k \cdot \nabla_k U \right)^2 \right\} \dots \end{aligned} \quad (2.4.8)$$

where w_1 vanishes during the integration because of the odd function of momenta. When Eqs.(2.4.8) are substituted into Eq.(2.4.6), Eq.(2.4.9) can be obtained.

$$Q_N = \frac{(2\pi m k_B T)^{3N/2}}{h^{3N}} \iint e^{-\beta U} \left\{ 1 - \frac{\hbar^2 \beta^2}{12m} \sum_{k=1}^N \left(\nabla_k^2 U - \frac{\beta}{2} (\nabla_k U)^2 \right) + \dots \right\} d\mathbf{r}_1 \dots d\mathbf{r}_N \quad (2.4.9)$$

By dividing Eq.(2.4.9) by $N!$ and substituting it into Eqs(2.4.10) and (2.4.11), we can get Eq(2.4.12).

$$Z_N = N! \left(\frac{V}{Q_1} \right)^N Q_N \quad (2.4.10)$$

$$B_2 = -b_2 = -\frac{1}{2V} (Z_2 - Z_1^2) \quad (2.4.11)$$

$$B_2 = -2\pi \int_0^{\infty} (e^{-\beta U(r)} - 1) r^2 dr + \frac{\hbar^2 \pi}{6m(k_B T)^3} \int_0^{\infty} \left(\frac{dU(r)}{dr} \right)^2 e^{-\beta U(r)} r^2 dr + O(\hbar^3) \quad (2.4.12)$$

The first term in Eq.(2.4.12) is the classical SVC, the second term is the first order quantum correction to the SVC and the small contribution coming from \hbar^3 term represents the quantum mechanical ideal gas SVC which is negligible.

2.5. Thermodynamic Properties

The basic thermodynamic relations are given in Eqs.(2.5.1). The formulae of the internal energy, enthalpy, entropy and Gibbs free energy are shown respectively (Kallmann, 1950).

$$\begin{aligned}
 E &= \int_0^T C_v dT \\
 H &= \int_0^T C_p dT \\
 S &= \int_0^T C_p \frac{dT}{T} \\
 F &= H - TS
 \end{aligned} \tag{2.5.1}$$

where C_p is constant pressure heat capacity and C_v is constant volume heat capacity. The pressure derivatives of thermodynamic properties can be given in Eqs.(2.5.2).

$$\begin{aligned}
 \left(\frac{\partial F}{\partial P}\right)_T &= V, \quad \left(\frac{\partial S}{\partial P}\right)_T = -\left(\frac{\partial V}{\partial T}\right)_P, \quad \left(\frac{\partial H}{\partial P}\right)_T = V - T\left(\frac{\partial V}{\partial T}\right)_P, \\
 \left(\frac{\partial E}{\partial P}\right)_T &= -P\left(\frac{\partial V}{\partial P}\right)_T - T\left(\frac{\partial V}{\partial T}\right)_P, \quad \left(\frac{\partial C_p}{\partial P}\right)_T = -T\left(\frac{\partial^2 V}{\partial T^2}\right)_P, \\
 \left(\frac{\partial C_v}{\partial P}\right)_T &= T\left(\frac{\partial^2 P}{\partial T^2}\right)_V \left(\frac{\partial V}{\partial P}\right)_T
 \end{aligned} \tag{2.5.2}$$

All thermodynamic properties can be derived in terms of the SVC, starting from the truncated virial equation of state for the real gases in Eq.(2.5.3).

$$PV = RT + B(T)P \tag{2.5.3}$$

The partial differentials used for the derivation of thermodynamic properties can be obtained using the Eq.(2.5.3) as following.

$$\begin{aligned}
\left(\frac{\partial V}{\partial T}\right)_P &= \frac{R}{P} + \frac{\partial B}{\partial T} \\
\left(\frac{\partial^2 V}{\partial T^2}\right)_P &= \frac{\partial^2 B}{\partial T^2} \\
\left(\frac{\partial V}{\partial P}\right)_T &= -\frac{RT}{P^2} = -\frac{(V-B)^2}{RT} \\
\left(\frac{\partial P}{\partial T}\right)_V &= \frac{R}{V-B} + \frac{RT}{(V-B)^2}
\end{aligned} \tag{2.5.4}$$

Noting that, the terms higher than $(V-B)^{-2}$ are neglected in Eq.(2.5.5).

$$\left(\frac{\partial^2 P}{\partial T^2}\right) = \frac{2V}{(V-B)^2} \frac{\partial B}{\partial T} + \frac{RT}{(V-B)^2} \frac{\partial^2 B}{\partial T^2} \tag{2.5.5}$$

The thermodynamic properties in terms of the SVC and its first and second derivatives can be obtained by using Eqs.(2.5.4) and (2.5.5) substituted into Eq.(2.5.2).

$$\Delta S = -R \ln P - \frac{B_1(T)P}{T} - \frac{(B(T))^2 P^2}{2RT^2} + \dots$$

$$\Delta H = P(B(T) - B_1(T) + \dots)$$

$$\Delta E = -PB_1(T) + \dots$$

$$\Delta F = RT \ln P + PB(T) + \dots \tag{2.5.6}$$

$$\Delta C_v = -\frac{P(2B_1(T) + B_2(T))}{T} - \frac{(B_1(T))^2 P^2}{RT^2} + \dots$$

$$\Delta C_p = -\frac{PB_2(T)}{T} + \dots$$

Eqs.(2.5.6) include Δ symbol meaning changes in enthalpy, entropy, internal energy, free energy and specific heat capacities and $B_1(T) = T \frac{dB(T)}{dT}$ and $B_2(T) = T^2 \frac{d^2B(T)}{dT^2}$.

As one of the thermodynamic properties, the speed of sound c can be represented in terms of the SVC and its derivatives as:

$$c^2 = \frac{\gamma RT}{M} \left(1 + \frac{P}{RT} \left(2B(T) + 2(\gamma - 1)B_1(T) + \frac{(\gamma - 1)^2}{\gamma} B_2(T) + \dots \right) \right) \quad (2.5.7)$$

where γ is the adiabatic constant, R is the gas constant and M is molecular mass of the gas.



3. METHODS AND RESULTS

3.1. A General Analytical Method for Evaluation of The Thermodynamic Properties of Matters Using Virial Coefficients with Morse Potential at High Temperature¹

The equation of state for imperfect gases is available in the literature as virial expansion in terms of density (Kaplan, 2006). The SVC is the first term in the expansion representing the first order deviation from the ideal gas, which is used for the calculations of thermodynamic properties of gases and partially ionized plasmas. In order to have an analytical calculation of SVC, various kinds of potentials are used for intermolecular interactions such as Lennard-Jones (Mamedov and Somuncu, 2014) Rydberg (Sinanoğlu and Pitzer, 1959), Mie (Heyes and Vasconcelos, 2017) and Morse (Matsumoto, 1987) e.c.t. for gases and plasmas. To our knowledge, the studies of the analytical evaluation approaches of the second virial coefficient with Morse potential are quite limited in the literature. Although Morse potential demonstrates more attraction for the long range interactions, it is preferred at high temperature studies ($T > 3000$ °K) since contributions of short range interactions are more significant at high temperatures. On the other hand, long range potentials such as Lennard-Jones (6-12) and modified Buckingham provide more accurate results at lower temperatures where plasmas can not exist (McQuarrie, 1976).

It is very important to have an accurate analytical solution of SVC for gases and also for neutral interactions of partially ionized plasma for the Generalized Chemical Model in order to achieve the exact values of thermodynamic properties of gases and plasmas. There are two general kinds of approaches in plasma physics to have equation of state which are physical and chemical methods. In the physical approach, electrons and protons are treated as fundamental particles, but atoms and molecules as compound species formed via fundamental particles' bounding process (Omarbakiyeva, 2010). The first principles approach simulations consider ions classically and electrons degenerate as a result of a quantum approach and combined quantum molecular dynamics and density functional theory together (Recoules et al., 2009). Average atom model also uses first principles method to describe electrons inside the spherical neutral cell with Wigner-Seitz radius to determine the properties of plasmas

¹ This chapter is a slightly modified version of our manuscript published in *Contributions to Plasma Physics* and has been reproduced here with the permission of the copyright holder.

(Johnson et al., 2006), but average atom, first principles and molecular dynamics methods are having difficulty when the density of the system is small since they are based on description of crystal systems (Apfelbaum, 2017). Depending on first principle approaches, fugacity expansion is given as an another example of physical approach which Ebeling used SVC during his calculations of plasmas in weak magnetic fields (Ebeling et al., 2000). All the components of partially ionized plasma (electrons, ions, neutral atoms and molecules) are considered as separate species within the Generalized Chemical Model (GCM) (allowing calculations at low density region), so that free energy can be evaluated as the sum of ideal, and interacting particles between charged-charged, neutral-charged and neutral-neutral. Apfelbaum considered plasmas with coupling parameter as $\Gamma \leq 1$, so that interactions are taken into account, but evaluated low density limit to avoid quantum effects and used Morse potential for SVC calculations of neutral particles during his calculations (Apfelbaum, 2013; Apfelbaum, 2016; Apfelbaum, 2017). Khomkin and Shumikhin also used chemical model but they preferred Lennard-Jones (6-12) potential for the SVC of neutrals (Khomkin and Shumikhin, 2014).

This study focuses on high temperature gas and partially ionized plasma investigation of neutral atom interactions through an analytical calculation of the second virial coefficient with preferably Morse potential which is used for many other purposes in the literature such as evaluation of the vibrational energy transfer for diatomic molecules (Calvert and Amme, 1966), crystal properties of solids (Girifalco and Weizer, 1958), bound state solutions of Schrödinger equation (Arda and Sever, 2011) and intermolecular forces in liquids (Mayer and Careri, 1952). The bound states are available if the temperature obeys $T < \frac{I}{10 k_B}$ (ionisation energy I values are acquired from the NIST atomic spectra database) approximate expression which all the tabulated SVC values of all atoms and molecules are calculated up to these values (Ebeling et al, 2017). Since noble gases have high ionization energy, their SVC results are taken up to high temperature values. The classical statistics formulas obtained for this study require considerable corrections at the low temperatures creating a low temperature application limit for this study with dimensionless temperature value suggested to be $T^* \geq 25$ ($T^* = T \frac{k_B}{D}$ where k_B is Boltzmann's constant and D is the potential well depth) in order to avoid quantum effects which have more influences on light gases such as He and H_2 (Lucas, 1991). For the heavier gases, contributions arising from quantum effects becomes much little and these gases tends to behave more classically at even more reduced temperature

values (Hryniewicki, 2011). In the literature, tabulated quantum correction values are provided for different potentials for down to $T^* = 0.3$ values which can be a good approximation for the other potentials (Hryniewicki, 2011; Boyd, 1970). In another study, Konowalow et al. calculated the SVC and its temperature derivatives and tabulated SVC values for the arbitrary values of the Morse parameter c (depending on curvature of the potential at the minimum) (Konowalow et al., 1961). Another analytical solution of SVC with Morse potential which focuses on obtaining the Morse parameters for different atoms and molecules and compares results with Lennard Jones (6-12) parameters (Matsumoto, 1987). Saxena and Gambhir applied a combination rule for the calculation of SVC of gaseous mixtures (Saxena and Gambhir, 1963).

In this study, an accurate analytical solution of SVC with Morse potential is obtained, applied to different atoms and molecules for up to the highest temperature that neutrals are still available and compared with both another analytical and numerical value and proved to provide reliable thermodynamic properties as well.

3.1.1. Analytical expression of SVC with Morse potential

The virial equation of state may be introduced in terms of a power series per volume as (Kunz and Kapner, 1969):

$$\frac{P\bar{V}}{RT} = Z = 1 + \frac{B(T)}{\bar{V}} + \frac{C(T)}{\bar{V}^2} + \dots \quad (3.1.1.1)$$

where Z is representing the compressibility factor, \bar{V} is the molar volume and $B(T)$ is the second virial coefficient depending on temperature and intermolecular potential function $U(r)$. The SVC is defined as:

$$B(T) = -2\pi N_A \int_0^\infty [e^{-U(r)/k_B T} - 1] r^2 dr \quad (3.1.1.2)$$

where N_A is Avogadro's number. An equivalent formula of SVC may be introduced as (Vargas et al., 2001):

$$B(T) = -\frac{2\pi N_A}{3k_B T} \int_0^\infty \frac{dU(r)}{dr} e^{-U(r)/k_B T} r^3 dr \quad (3.1.1.3)$$

Before introducing related thermodynamic functions, a unit conversion of $B(T)$ is necessary to convert SVC units from cm^3/mol to $\text{cal}/\text{mol}\cdot\text{atm}$ ($1 \text{ cal} = 4.13 \times 10^{-2} \text{ L}\cdot\text{atm}$). The

velocity of sound in different substances is one of the thermodynamic properties that can be calculated using the SVC with Morse potential of this study as an application by using the following formula (Hirschfelder et al., 1954):

$$c_0^2 = \frac{\gamma RT}{M} \left[1 + \frac{P}{RT} \left(2B(T) + 2(\gamma - 1)B_1(T) + \frac{(\gamma-1)^2}{\gamma} B_2(T) \right) + \dots \right] \quad (3.1.1.4)$$

where P is the pressure, $B_1(T) = T \frac{dB(T)}{dT}$ and $B_2(T) = T^2 \frac{d^2B(T)}{dT^2}$. Since the last two terms including $B_1(T)$ and $B_2(T)$ in Eq.(3.1.1.4) contribute very little for the given data range in Table 5, they will be neglected during calculations. γ, M and ideal speed of sound values c_{0i} are acquired from The NASA Computer program CEA (Chemical Equilibrium with Applications) (CEARUN NASA, retrieved 2018).

For the calculation of SVC with the Morse potential where its first exponential expression represents the repulsive forces due to the Pauli Exclusion Principle and the second one stands for the attractive forces between atoms and defined as (Al-Maaitah, 2018):

$$U(r) = D \{ \exp[-2\alpha(r - r_e)] - 2\exp[-\alpha(r - r_e)] \} \quad (3.1.1.5)$$

Where D is the potential well depth, r_e is equilibrium distance and α represents the potential's curvature at its minimum. In order to reconstruct Eq. (3.1.1.3), new expressions are offered in Eqs.(3.1.1.6) and Eq. (3.1.1.7) obtained in literature (Matsumoto, 1987):

$$p = \frac{D}{k_B T}, \quad b = \sqrt{p} \exp(\alpha r_e), \quad x = b \exp(-\alpha r). \quad (3.1.1.6)$$

With the new definitions, the SVC may be introduced as following

$$B(T) = \frac{4\pi N_A}{3\alpha^3} \int_0^b (\sqrt{p} - x) \left(e^{-x^2 + 2x\sqrt{p}} \right) \left(\ln \frac{x}{b} \right)^3 dx \quad (3.1.1.7)$$

For the analytical solution of Eq. (3.1.1.7), an alternative approach is applied by using a third power binomial expansion theorem.

$$\begin{aligned}
B(T) = \frac{4\pi N_A}{3\alpha^3} & \left\{ 3(\ln b)^2 \sqrt{p} \int_0^b e^{-x^2+2x\sqrt{p}} \ln x dx - 3(\ln b)^2 \int_0^b x e^{-x^2+2x\sqrt{p}} \ln x dx + \sqrt{p} \int_0^b e^{-x^2+2x\sqrt{p}} (\ln x)^3 dx \right. \\
& - \int_0^b x e^{-x^2+2x\sqrt{p}} (\ln x)^3 dx - 3 \ln b \sqrt{p} \int_0^b e^{-x^2+2x\sqrt{p}} (\ln x)^2 dx + 3 \ln b \int_0^b x e^{-x^2+2x\sqrt{p}} (\ln x)^2 dx \\
& \left. - (\ln b)^3 \sqrt{p} \int_0^b e^{-x^2+2x\sqrt{p}} dx + (\ln b)^3 \int_0^b x e^{-x^2+2x\sqrt{p}} dx \right\} \quad (3.1.1.8)
\end{aligned}$$

The following exponential series expansion formula is used for the term $e^{2x\sqrt{p}}$ in Eq.(3.1.1.8):

$$e^{\pm x} = \sum_{i=0}^{\infty} (\pm 1)^i \frac{x^i}{i!} . \quad (3.1.1.9)$$

After substituting Eq. (3.1.1.9) into Eq. (3.1.1.8), we have obtained a general analytical formula for the SVC with Morse potential as:

$$B(T) = \frac{4\pi N_A 10^{-24}}{3\alpha^3} \{K(p,b) + L(p,b) + M(p,b) + N(p,b) + P(p,b) + R(p,b) + S(p,b) + V(p,b)\} \quad (3.1.1.10)$$

where 10^{-24} arises from the unit conversion of $1 \text{ \AA}^3 = (10^{-8})^3 \text{ cm}^3$ and the analytical solutions of eight integrals appearing in Eq.(3.1.1.8) are given in the same order in Eq.(3.1.1.10). In Eq.(3.1.1.10), the quantities $K(p,b)$, $L(p,b)$, $M(p,b)$, $N(p,b)$, $P(p,b)$, $R(p,b)$, $S(p,b)$ and $V(p,b)$ are defined as, respectively:

$$K(p,b) = 3\sqrt{p} (\ln b)^2 \sum_{i=0}^n \frac{C(i,b)}{i!} (2\sqrt{p})^i \quad (3.1.1.11)$$

$$L(p,b) = -3(\ln b)^2 \sum_{i=0}^n \frac{C(i+1,b)}{i!} (2\sqrt{p})^i \quad (3.1.1.12)$$

$$M(p,b) = \sqrt{p} \sum_{i=0}^n \frac{D(i,b)}{i!} (2\sqrt{p})^i \quad (3.1.1.13)$$

$$N(p,b) = -\sum_{i=0}^n \frac{D(i+1,b)}{i!} (2\sqrt{p})^i \quad (3.1.1.14)$$

$$P(p,b) = -3\ln b \sqrt{p} \sum_{i=0}^n \frac{F(i,b)}{i!} (2\sqrt{p})^i \quad (3.1.1.15)$$

$$R(p,b) = 3\ln b \sum_{i=0}^n \frac{F(i+1,b)}{i!} (2\sqrt{p})^i \quad (3.1.1.16)$$

$$S(p,b) = -\sqrt{p} (\ln b)^3 \left(\frac{1}{2} e^p \sqrt{\pi} \left(\text{Erf}(b-\sqrt{p}) + \text{Erf}(\sqrt{p}) \right) \right) \quad (3.1.1.17)$$

$$V(p,b) = (\ln b)^3 \left(\frac{1}{2} \left(1 - e^{-b(b-2\sqrt{p})} + e^p \sqrt{p\pi} \left(\text{Erf}(b-\sqrt{p}) + \text{Erf}(\sqrt{p}) \right) \right) \right) \quad (3.1.1.18)$$

In Eqs. (3.1.1.11), (3.1.1.12), (3.1.1.13), (3.1.1.14), (3.1.1.15) and (3.1.1.16), the general functions of C , D and F are introduced as:

$$C(n,b) = -\frac{1}{4} \left(2\Gamma\left(\frac{n+1}{2}, b^2\right) \ln b + G_{2,3}^{3,0} \left(b^2 \middle| \begin{matrix} 1, & 1 \\ 0, & 0, & \frac{n+1}{2} \end{matrix} \right) + \Gamma\left(\frac{n+1}{2}\right) \left(-2\ln b + \ln b^2 - \psi^{(0)}\left(\frac{n+1}{2}\right) \right) \right) \quad (3.1.1.19)$$

$$\begin{aligned}
D(n, b) = & \frac{1}{16} \left(8\Gamma\left(\frac{n+1}{2}\right)(\ln b)^3 - 8\Gamma\left(\frac{n+1}{2}, b^2\right)(\ln b)^3 - 12\Gamma\left(\frac{n+1}{2}\right)(\ln b)^2 \ln b^2 + 6\Gamma\left(\frac{n+1}{2}\right) \ln b (\ln b^2)^2 - \right. \\
& \Gamma\left(\frac{n+1}{2}\right)(\ln b^2)^3 - 12(\ln b)^2 G_{2,3}^{3,0} \left(b^2 \middle| \begin{matrix} 1, & 1 \\ 0, & 0, & \frac{n+1}{2} \end{matrix} \right) - 12 \ln b G_{3,4}^{4,0} \left(b^2 \middle| \begin{matrix} 1, & 1, & 1 \\ 0, & 0, & 0, & \frac{n+1}{2} \end{matrix} \right) - \\
& 6G_{4,5}^{5,0} \left(b^2 \middle| \begin{matrix} 1, & 1, & 1, & 1 \\ 0, & 0, & 0, & 0, & \frac{n+1}{2} \end{matrix} \right) + 3\Gamma\left(\frac{n+1}{2}\right) (-2 \ln b + \ln b^2)^2 \psi^{(0)}\left(\frac{n+1}{2}\right) + 6\Gamma\left(\frac{n+1}{2}\right) \ln b \left(\psi^{(0)}\left(\frac{n+1}{2}\right) \right)^2 - \\
& 3\Gamma\left(\frac{n+1}{2}\right) \ln b^2 \left(\psi^{(0)}\left(\frac{n+1}{2}\right) \right)^2 + \Gamma\left(\frac{n+1}{2}\right) \left(\psi^{(0)}\left(\frac{n+1}{2}\right) \right)^3 + 3\Gamma\left(\frac{n+1}{2}\right) (2 \ln b - \ln b^2) \psi^{(1)}\left(\frac{n+1}{2}\right) + \\
& \left. 3\Gamma\left(\frac{n+1}{2}\right) \psi^{(0)}\left(\frac{n+1}{2}\right) \psi^{(1)}\left(\frac{n+1}{2}\right) + \Gamma\left(\frac{n+1}{2}\right) \psi^{(2)}\left(\frac{n+1}{2}\right) \right) \quad (3.1.1.20)
\end{aligned}$$

$$\begin{aligned}
F(n, b) = & \frac{1}{8} \left(4\Gamma\left(\frac{n+1}{2}\right)(\ln b)^2 - 4\Gamma\left(\frac{n+1}{2}, b^2\right)(\ln b)^2 - 4\Gamma\left(\frac{n+1}{2}\right) \ln b \ln b^2 + \right. \\
& \Gamma\left(\frac{n+1}{2}\right)(\ln b^2)^2 - 4 \ln b G_{2,3}^{3,0} \left(b^2 \middle| \begin{matrix} 1, & 1 \\ 0, & 0, & \frac{n+1}{2} \end{matrix} \right) - 2G_{3,4}^{4,0} \left(b^2 \middle| \begin{matrix} 1, & 1, & 1 \\ 0, & 0, & 0, & \frac{n+1}{2} \end{matrix} \right) + \\
& \left. 2\Gamma\left(\frac{n+1}{2}\right) (2 \ln b - \ln b^2) \psi^{(0)}\left(\frac{n+1}{2}\right) + \Gamma\left(\frac{n+1}{2}\right) \left(\psi^{(0)}\left(\frac{n+1}{2}\right) \right)^2 + \Gamma\left(\frac{n+1}{2}\right) \psi^{(1)}\left(\frac{n+1}{2}\right) \right) \quad (3.1.1.21)
\end{aligned}$$

where gamma, incomplete gamma, digamma and Meijer G functions appear in Eqs. (3.1.1.19), (3.1.1.20) and (3.1.1.21) and polygamma functions are introduced in Eqs. (3.1.1.20) and (3.1.1.21) may be defined as respectively (Gradshteyn and Ryzhik, 1965):

$$\Gamma(a) = \int_0^{\infty} t^{a-1} e^{-t} dt \quad (3.1.1.22)$$

$$\Gamma(a, x) = \int_x^{\infty} t^{a-1} e^{-t} dt \quad (3.1.1.23)$$

$$\psi_0(z) = \frac{d}{dz} \ln \Gamma(z) = \frac{\Gamma'(z)}{\Gamma(z)} \quad (3.1.1.24)$$

$$G_{p,q}^{m,n} \left(z \middle| \begin{matrix} a_1, \dots, a_p \\ b_1, \dots, b_q \end{matrix} \right) = \frac{1}{2\pi i} \int_L \frac{\prod_{j=1}^m \Gamma(b_j - s) \prod_{j=1}^n \Gamma(1 - a_j + s)}{\prod_{j=m+1}^q \Gamma(1 - b_j + s) \prod_{j=n+1}^p \Gamma(a_j - s)} z^s ds \quad (3.1.1.25)$$

$$\psi_n(z) = \frac{d^{n+1}}{dz^{n+1}} \ln(\Gamma(z)) = \frac{d^n}{dz^n} \frac{\Gamma'(z)}{\Gamma(z)} = \frac{d^n}{dz^n} \psi_0(z) \quad (3.1.1.26)$$

3.1.2. Computational results of established formula and its application

The SVC values of some atoms and molecules for different temperatures, crucial for the evaluation of the thermodynamical properties of gases and the generalized chemical model of partially ionized plasmas, are acquired for this study as an application to real gases by using Eq. (3.1.1.10). Tables 3.2-3.4 introduces the SVC values of corresponding temperature in each row with three results for every atom or molecule that the first one stands for the analytical result of Eq. (3.1.1.10), the second one represents the analytical result of literature (Matsumoto, 1987) and the third one is the numerical result of the SVC with Morse potential for noble gases of *He*, *Ne*, *Ar*, *Kr* and *Xe*, semiconductors *B*, *Si* and metal *Zn* and molecules of *H₂*, *N₂*, *O₂*, *NO*, *CO*, respectively. Noting that, a useful approach given in the literature (Matsumoto, 1987), with the analytical formula was established under assumption for $b \rightarrow \infty$. This corresponds to lower temperatures which provides very practical and accurate results at this temperature region. The main advantage of our established formula is its validity for arbitrary values of parameter b leading to evaluation of the SVC for all temperature ranges.

During the calculations, Morse parameters appeared in Eq. (3.1.1.5) are introduced for each atom and molecule in Table 3.1. Figs. 3.1-3.3 demonstrates the analytical SVC values with Morse potential using Eq. (3.1.1.10) for different temperatures for noble gases of *He*, *Ne*, *Ar*, *Kr* and *Xe*, semiconductors *B*, *Si* and metal *Zn* and molecules of *H₂*, *N₂*, *O₂*, *NO*, *CO*, respectively. The noble gases results from Table 3.2 display the exact match between the two analytical methods and differ very slightly from the numerical results that the maximum percent error found to be % 0.0074 for *He* gas at 21000 °K, proving the accuracy of the new analytical method. The results of *B*, *Si* and *Zn* from Table 3.3 demonstrate the equal analytical results except for *Si* at 4000 °K and 7000 °K, which results from Eq. (3.1.1.10) for *Si* display closer values (or exact for 7000 °K) to the numerical results. Table 3.3 also displays another fact that three results for each temperature value can be distinguished easily at lower decimal places when the values of b and p (from Eq.(3.1.1.6)) are high such as *B* and *Si* results. When the Table 3.4 examined, only the two analytical data for *O₂* at 5000 °K

and 6000 °K differ slightly from each other and values from literature (Matsumoto, 1987) are closer to the numerical values.

As an application, the three speed of sound values for each temperature are calculated for *Zn*, *Ar* and *N₂* for the temperature range between 3000-7000 °K in Table 3.5. The first obtained c_0 value is for 0.1 atm and the second one is for 1 atm that demonstrates the deviation from the ideal gas behavior except for *Zn* at 3000-6000 °K temperature range. In this temperature region of *Zn*, the SVC is negative indicating the existence of dominant intermolecular attractive forces resulting in pressure decline compared to that acquired values using ideal gas law (Lucas, 1991). The results are compared with ideal speed of sound data from NASA chemical equilibrium with applications and found to be in a good agreement between them, ensuring that the obtained analytical formula is convenient for acquiring the further thermodynamic properties.

After providing an analytical solution to the SVC over Morse potential, it has been applied to some atoms and molecules for different temperature values for the application by using Mathematica 7.0 software. The values of SVC with Morse potential of another analytical solution from the literature and numerical values are calculated and tabulated for the comparison. It has been proved that the new analytical solution provides us accurate analytical SVC and speed of sound results being in a good agreement with compared results from literature and operates precisely at any arbitrary temperature value.

Table 3.1. Morse potential parameters are obtained from literature for *Zn* (Apfelbaum, 2017), for *B* and *Si* (Apfelbaum, 2013) and the remaining from literature (Matsumoto, 1987).

	D/k_B °K	r_e Å	α Å ⁻¹
<i>He</i>	12.6	2.92	2.197
<i>Ne</i>	51.3	3.09	2.036
<i>Ar</i>	118.1	4.13	1.253
<i>Kr</i>	149.0	4.49	1.105
<i>Xe</i>	226.9	4.73	1.099
<i>B</i>	32144.478	1.59	1.962
<i>Si</i>	37946.731	2.246	1.438
<i>Zn</i>	522.203	1.19	2.9496
<i>H₂</i>	49.4	3.29	1.923
<i>N₂</i>	93.4	4.43	1.166
<i>O₂</i>	152.4	3.75	1.542
<i>CO</i>	100.3	4.27	1.136
<i>NO</i>	131.8	4.22	1.309

Table 3.2. The first result in each box is the analytical result of Eq. (3.1.1.10), the second one is the analytical result of the literature (Matsumoto,1987) and the third one is the numerical result of the SVC with Morse potential for the noble gases of *He, Ne, Ar, Kr* and *Xe* for different temperatures.. All the $B(T)$ results in Tables 3.2-3.5 are in $\text{cm}^3 \cdot \text{mol}^{-1}$ units.

$T(^{\circ}K)$	<i>He</i>	<i>Ne</i>	<i>Ar</i>	<i>Kr</i>	<i>Xe</i>
3000					35.9486494 35.9486494 35.9486492
4000				27.7713544 27.7713544 27.7713543	36.5717095 36.5717095 36.5717091
5000				26.9053877 26.9053877 26.9053876	36.2883854 36.2883854 36.2883855
6000			20.9185322 20.9185322 20.9185321	26.0026119 26.0026119 26.0026119	35.6801636 35.6801636 35.6801635
7000			20.1275058 20.1275058 20.1275055	25.1354372 25.1354372 25.1354371	34.9566325 34.9566325 34.9566324
8000		9.19066093 9.19066093 9.19066084	19.4132444 19.4132444 19.4132442	24.3247278 24.3247278 24.3247277	34.2037308 34.2037308 34.2037308
9000		8.87889049 8.87889049 8.87889041	18.7668436 18.7668436 18.7668436	23.5738170 23.5738170 23.5738170	33.4590529 33.4590529 33.4590527
10000	4.65901985 4.65901985 4.65901666	8.60194506 8.60194506 8.60194876	18.1793251 18.1793251 18.1793252	22.8798761 22.8798761 22.8798761	32.7392050 32.7392050 32.7392049
11000	4.48955651 4.48955651 4.48955333	8.35339003 8.35339003 8.35338997	17.6427123 17.6427123 17.6427124	22.2380999 22.2380999 22.2380999	32.0510383 32.0510383 32.0510382
12000	4.33797783 4.33797783 4.33797553	8.12837996 8.12837996 8.12837990	17.1502085 17.1502085 17.1502086	21.6433209 21.6433209 21.6433200	31.3966814 31.3966814 31.3966814
13000	4.20120210 4.20120210 4.20120209	7.92318218 7.92318218 7.92318212	16.6961033 16.6961033 16.6961033	21.0906271 21.0906271 21.0906272	30.7759434 30.7759434 30.7759434
14000	4.07685942 4.07685942 4.07685940	7.73486469 7.73486469 7.73486464	16.2756117 16.2756117 16.2756116	20.5755723 20.5755723 20.5755724	30.1875140 30.1875140 30.1875140
15000	3.96309080 3.96309080 3.96309077	7.56108535 7.56108535 7.56108530	15.8847157 15.8847157 15.8847157	20.0942198 20.0942198 20.0942198	29.6295818 29.6295818 29.6295818
16000	3.85841299 3.85841299 3.85841296	7.39994552 7.39994552 7.39994548	15.5200256 15.5200256 15.5200255	19.6431172 19.6431172 19.6431172	

Table 3.2. (Continuous) The first result in each box is the analytical result of Eq. (3.1.1.10), the second one is the analytical result of the literature (Matsumoto,1987) and the third one is the numerical result of the SVC with Morse potential for the noble gases of *He, Ne, Ar, Kr* and *Xe* for different temperatures.. All the $B(T)$ results in Tables 3.2-3.5 are in $\text{cm}^3 \cdot \text{mol}^{-1}$ units.

17000	3.76162495 3.76162495 3.76162492	7.24988617 7.24988617 7.24988613	15.1786657 15.1786657 15.1786656	19.2192479 19.2192479 19.2192479	
18000	3.67174148 3.67174148 3.67174145	7.10961242 7.10961242 7.10961238	14.8581819 14.8581819 14.8581819		
19000	3.58794516 3.58794516 3.58794514	6.97803778 6.97803778 6.97803775	14.5564674 14.5564674 14.5564674		
20000	3.50955089 3.50955089 3.50955088	6.85424232 6.85424232 6.85424229			
21000	3.43597917 3.43597917 3.43572596	6.73744067 6.73744067 6.73744064			
22000	3.36673581 3.36673581 3.36673581	6.62695737 6.62695737 6.62695733			
23000	3.30139625 3.30139625 3.30139625	6.52220751 6.52220751 6.52220746			
24000	3.23959323 3.23959323 3.23959323	6.42268146 6.42268146 6.42268139			
25000	3.18100714 3.18100714 3.18100714	6.32793268 6.32793268 6.32793259			
26000	3.12535823 3.12535823 3.12535824				
27000	3.07240037 3.07240037 3.07240037				
28000	3.02191594 3.02191594 3.02191595				
29000	2.97371171 2.97371171 2.97371171				

Table 3.3. The SVC results with Morse potential for semiconductors *B* and *Si* and a metal *Zn* for different temperatures (in units of $\text{cm}^3 \cdot \text{mol}^{-1}$). The data order is the same as Table 3.2.

<i>T</i> (°K)	<i>B</i>	<i>Si</i>	<i>Zn</i>
3000			-0.4260046839 -0.4260046839 -0.4260046830
4000	-11117.56202 - 11117.56202 -11117.56175	-114758.18272 -114758.18295 -114758.18241	-0.20409416099 - 0.20409416099 -0.20409416072
5000	-2632.43424 -2632.43424 -2632.43417	-20107.87978 -20107.87978 -20107.87937	-0.08399215083 -0.08399215083 -0.08399215063
6000	-1039.90451 -1039.90451 -1039.90742	-6506.85868 -6506.85868 -6506.85837	-0.01152871933 -0.01152871933 -0.01152871917
7000	-545.26640 -545.26640 -545.26883	-2970.98960 -2970.99320 -2970.98960	0.03528301237 0.03528301237 0.03528301250
8000	-338.88353 -338.88353 -338.88354	-1672.42072 -1672.42072 -1672.42063	0.06694048142 0.06694048142 0.06694048154
9000	-234.80665 -234.80665 -234.80666	-1077.48480 -1077.48480 -1077.48477	0.0890358175 0.0890358175 0.0890358173
10000	-175.05970 -175.05970 -175.05970	-760.50421 -760.50421 -760.50424	0.104793783 0.104793783 0.104793777
11000		-572.350416 -572.350416 -572.350440	0.1161892485 0.1161892485 0.1161892379

Table 3.4. The SVC results (in units of $\text{cm}^3 \cdot \text{mol}^{-1}$) with Morse potential for the molecules of H_2 , N_2 , O_2 , NO and CO for different temperatures. The data order is the same as Table 3.2.

$T(^{\circ}K)$	H_2	N_2	O_2	CO	NO
3000					28.65738215 28.65738215 28.65738224
4000					27.71234964 27.71234964 27.71234977
5000			20.69163013 20.67873806 20.67874537		26.71583362 26.71583362 26.71583362
6000	12.00716902 12.00716902 12.00716879	24.22172893 24.22172893 24.22172890	20.05344948 20.05324495 20.05310004	19.33848082 19.33848082 19.33848090	25.77737605 25.77737605 25.77737604
7000	11.50990765 11.50990765 11.50990744	23.18612419 23.18612419 23.18612416	19.46881920 19.46881920 19.46882447	18.48583473 18.48583473 18.48583482	24.91834190 24.91834190 24.91834192
8000	11.08067387 11.08067387 11.08067369	22.26909846 22.26909846 22.26909627	18.93010686 18.93010686 18.93011141	17.72496125 17.72496125 17.72496129	24.13705955 24.13705955 24.13705956
9000	10.70435223 10.70435223 10.70435209	21.45079662 21.45079662 21.45079669	18.43496634 18.43496634 18.43497026	17.04270880 17.04270880 17.04270879	23.42591050 23.42591050 23.42591049
10000	10.37023632 10.37023632 10.37023619	20.71498260 20.71498260 20.71498271	17.97932967 17.97932967 17.97933306	16.42731422 16.42731422 16.42731418	22.77639301 22.77639301 22.77639296
11000	10.07049292 10.07049292 10.07049280	20.04863994 20.04863994 20.04863994	17.55886419 17.55886419 17.55886717	15.86889401 15.86889401 15.86889396	22.18064065 22.18064065 22.18063426
12000	9.79923267 9.79923267 9.79923256	19.44134062 19.44134062 19.44134070	17.16953463 17.16953463 17.16953734	15.35929966 15.35929966 15.35929961	21.63179822 21.63179822 21.63179812
13000	9.55192432 9.55192432 9.55192422	18.88467802 18.88467802 18.88467807	16.80776328 16.80776328 16.80776588	14.89183464 14.89183464 14.89183460	
14000	9.32501217 9.32501217 9.32501207	18.37181543 18.37181543 18.37181544	16.47044112 16.47044112 16.47044374	14.46097784 14.46097784 14.46097781	
15000	9.11565818 9.11565818 9.11566080	17.89713997 17.89713997 17.89713995	16.15488670 16.15488670 16.15488943	14.06215012 14.06215012 14.06215009	
16000	8.92156334 8.92156334 8.92156325	17.45600011 17.45600011 17.45600006		13.69152683 13.69152683 13.69152680	
17000	8.74084095 8.74084095 8.74084087	17.04450627 17.04450627 17.04450622		13.34589015 13.34589015 13.34589011	
18000	8.57192479 8.57192479 8.57192471	16.65937860 16.65937860 16.65937854			
19000		16.29782962 16.29782962 16.29782956			

Table 3.5. The speed of sound calculations for *Ar*, *N₂* and *Zn* by using Eq. (3.1.1.4) for temperature range 3000- 7000 K. The first value of c_0 is calculated for $P = 0.1$ atm and the second one for $P = 1$ atm for each temperature and atom or molecule.

	$T(^{\circ}K)$	$B(T) \left(\frac{cm^3}{mol} \right)$ from Eq.(3.1.1.10)	$c_0(m/s)$ from Eq. (3.1.1.4)	$c_{0i} (m/s)^*$	$\gamma^* = \frac{C_P}{C_V}$	$M \left(\frac{g}{mol} \right)^*$
Ar	3000	23.6623759	1020.52 1021.41	1020.1	1.6667	39.948
	4000	22.7401176	1178.37 1179.10	1177.9	1.6667	39.948
	5000	21.7989151	1317.44 1318.07	1317.0	1.6667	39.948
	6000	20.9185322	1443.16 1443.71	1442.7	1.6667	39.948
	7000	20.1275058	1558.78 1559.27	1558.3	1.6667	39.948
N₂	3000	28.20951488	1071.55 1072.66	1071.1	1.2885	28.013
	4000	26.74266023	1212.01 1212.89	1211.6	1.2330	27.936
	5000	25.40735099	1327.69 1328.43	1327.3	1.1284	26.63
	6000	24.22172893	1638.86 1639.58	1638.3	1.1169	20.759
	7000	23.18612419	2099.50 2100.26	2098.8	1.1521	15.222
Zn	3000	-0.4260046839	797.530 797.517	797.3	1.6665	65.39
	4000	-0.20409416099	919.780 919.770	919.5	1.6624	65.39
	5000	-0.08399215083	1020.860 1020.858	1020.6	1.6383	65.39
	6000	-0.01152871933	1097.7313 1097.7310	1097.4	1.5786	65.39
	7000	0.03528301237	1153.3992 1153.3998	1153.1	1.4938	65.39

*Data are taken from CEARUN, NASA.

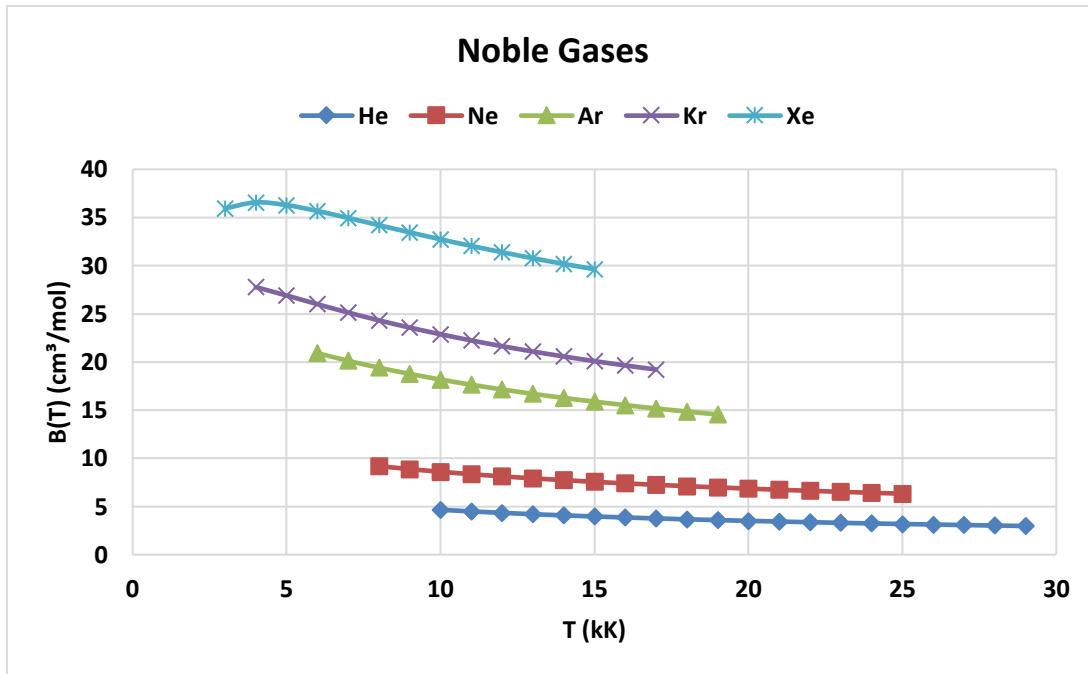


Figure 3.1. Dependence of the SVC with Morse potential (Eq. (3.2.9)) on temperature for *He*, *Ne*, *Ar*, *Kr* and *Xe*.

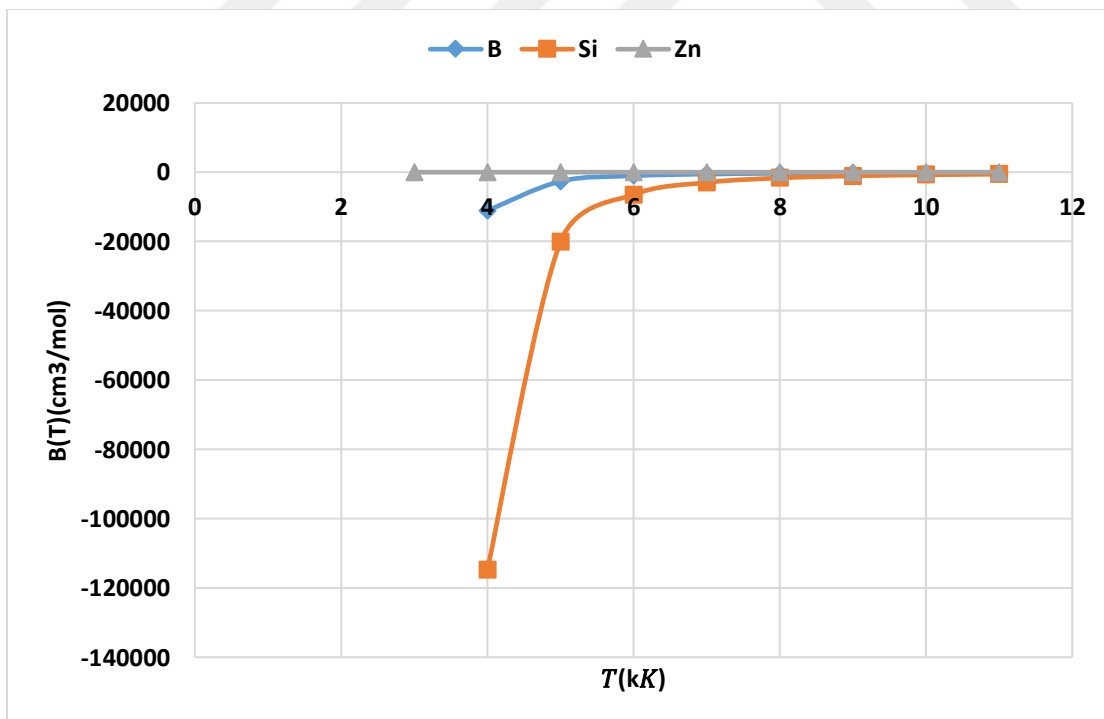


Figure 3.2. Dependence of the SVC with Morse potential (Eq.(3.2.9)) on temperature for *B*, *Si* and *Zn*.

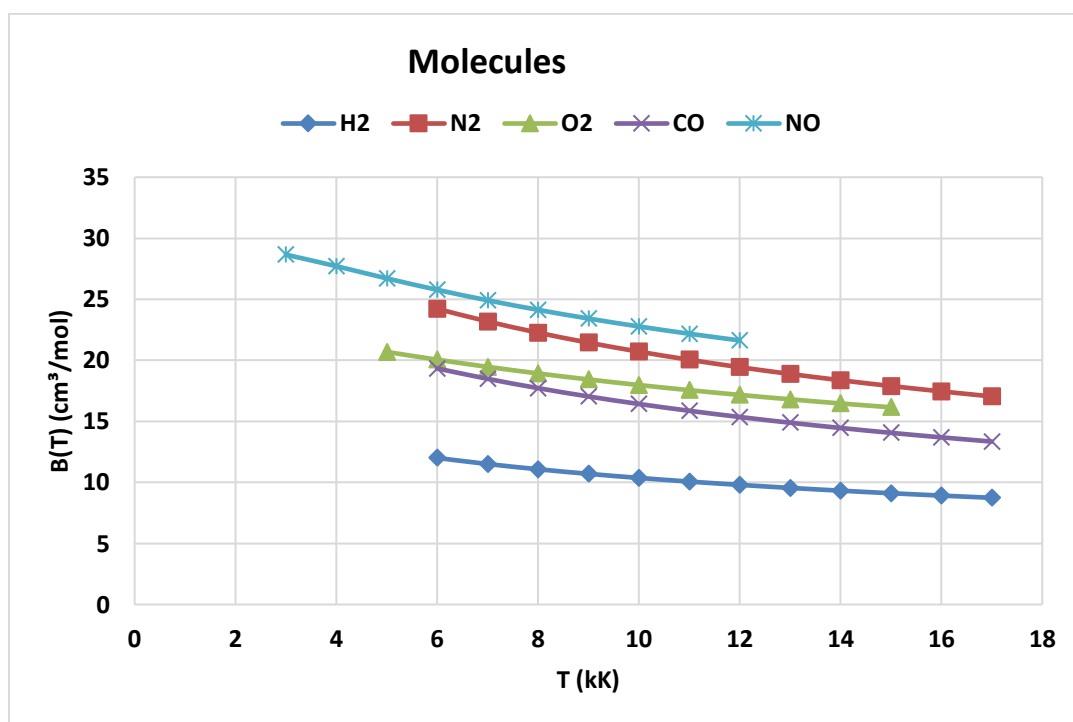


Figure 3.3. Dependence of the SVC with Morse potential (Eq.(3.2.9)) on temperature for the molecules of H_2 , N_2 , O_2 , NO and CO .

3.2. The Comparative Analytical Evaluation of Quantum Corrections to The Second Virial Coefficient with Morse Potential and Its Applications to Real Systems²

Virial coefficients with various potentials, playing significant role to determine intermolecular interactions, thermodynamic and transport properties of the gases and liquids, require some corrections at low temperature range where quantum effects are gradually increasing with decreasing temperature (McQuarrie, 1976; Landau and Lifshitz, 1980). Especially, the virial coefficients with Morse potential are very important in the evaluation of the thermodynamic and transport properties of gases and plasmas (Matsumoto, 1987; Apfelbaum, 2013; Apfelbaum, 2016; Apfelbaum, 2017). Also, the significant studies have been carried out on the investigation of drug design and DNA end-to-end stacking interactions by using second virial coefficients over the recent decades (Li et al., 2008). It is specifically emphasized that intermolecular potential energy surface obtained by using Hartree-Fock theory for drug

² This chapter is a slightly modified version of our manuscript published in *The Journal of Chemical Thermodynamics* and has been reproduced here with the permission of the copyright holder.

interactions with specific atoms creates satisfying results with SVC results especially with the Morse potential (Monajjemi et al., 2012). Noting that, analytical evaluation methods of the classical virial coefficients with Morse potential carried out so far is very limited (Konowalow et al., 1961; Matsumoto, 1987). In this sense, the obtained formula in the study (Matsumoto, 1987) is very useful approximation for the calculation of the thermodynamic properties of gases. However, classical SVC results need a quantum correction term at low temperatures where more significant effects have been observed at light molecules such as *He* and *H₂* (Hryniewicki, 2011). In the literature, numerous analytical methods for the quantum corrections of SVC with different potentials for both isotropic and anisotropic interactions exist such as Lennard-Jones (12-6) (Mamedov and Somuncu, 2016), Stockmayer (McCarty and Babu, 1970), Berns and van der Avoird (Corbin et al., 1984). Besides, one of the numerical methods of adaptive grids using polynomial interpolants of different degree is used for the quantum corrections to SVC with the Lennard-Jones (12-6), Rice and Hirschfelder modified Buckingham (exponential-six) and Buckingham and Corner modified Buckingham (Hryniewicki, 2011). An analytical evaluation attempt to classical and quantum corrections of second virial coefficient (SVC) with Morse potential have been analyzed in work (Bruch, 1967) to our knowledge. In the study (Bruch, 1967), the proposed approach for the first quantum correction of SVC with Morse potential was evaluated by using the Laplace transforms and applied to only *He* gas above 100 °K. As stated by the author, this approximate solution to both classical and first quantum correction of SVC with Morse potential is limited in the application since the approximation is only valid for certain range of temperature and potential parameters of certain molecules.

In this study, we have proposed an efficient analytical formula for the evaluation of the quantum correction of SVC with Morse potential and applied it to isotropic interactions. As seen from calculation results, the obtained formulae are useful for accurate evaluation of quantum correction of SVC with wide range of thermodynamic parameters. As an application, the correctness of the obtained results for the quantum correction of SVC with Morse has been compared with Lennard- Jones (12-6) potential data (Somuncu et al., 2019) and the classical SVC with Morse (Matsumoto, 1987) and Lennard- Jones (12-6) (Mamedov and Somuncu, 2014) calculations are included to display the significance of quantum correction effects on classical SVC results.

3.2.1. Analytical expressions of quantum correction to SVC with Morse potential

$B^0(T)$ is defined as classical SVC and the remaining terms represent the quantum corrections, the SVC can be given as a series expansion (Boyd, 1970):

$$B(T) = B^0(T) + qB^1(T) + q^2B^2(T) + \dots \quad (3.2.1.1)$$

where $q = \hbar^2/m$ and m is the mass of molecule. The first two terms in Eq.(3.2.1.1) can be given (Uhlenbeck and Beth, 1936):

$$B(T) = -2\pi N_A \int_0^\infty \left(e^{-U(r)/k_B T} - 1 \right) r^2 dr + \frac{\hbar^2 \pi N_A}{6m(k_B T)^3} \int_0^\infty \left(\frac{dU(r)}{dr} \right)^2 e^{-U(r)/k_B T} r^2 dr \quad (3.2.1.2)$$

where $U(r)$ is intermolecular interaction potential, N_A is Avagadro's number, \hbar is reduced Planck constant and k_B is Boltzmann's constant.

In this study, intermolecular interaction potential $U(r)$ is the Morse potential and defined as (Kaplan, 2006):

$$U(r) = D \{ \exp[-2\alpha(r - r_e)] - 2\exp[-\alpha(r - r_e)] \} \quad (3.2.1.3)$$

In order to solve the first quantum correction to SVC with Morse potential, we need to use some dimensionless parameters introduced in literature (Matsumoto, 1987) as following

$$p = \frac{D}{k_B T}, \quad b = \sqrt{p} \exp(\alpha r_e), \quad x = b \exp(-\alpha r). \quad (3.2.1.4)$$

By substituting Eq.(3.2.1.3) into Eq.(3.2.1.2) and using expressions in Eq.(3.2.1.4), we obtain the first quantum correction to SVC with Morse potential (second terms in Eq.(3.2.1.1) and (3.2.1.2)) as divided by Van der Waals value of $b_0 = \frac{2\pi N_A \sigma^3}{3}$ (in cm^3/mol units) and dimensionless quantum mechanical parameter $\Lambda^* = \hbar / \sigma \sqrt{mD}$ given as (Hirschfelder et al., 1954):

$$B^{*1}(T) = \frac{qB^1(T)}{\Lambda^{*2} b_0} = \frac{p}{16\pi^2 c} \int_0^b 4x (\sqrt{p} - x)^2 \left(e^{-x^2 + 2x\sqrt{p}} \right) \left(\ln \frac{x}{b} \right)^2 dx \quad (3.2.1.5)$$

where a new constant is introduced as $c = \sigma \alpha$ that σ is the distance where the potential becomes zero. In order to solve $B^{*1}(T)$, two second order binomial expansions are utilized for Eq.(3.2.1.5).

$$\begin{aligned}
B^{*1}(T) = & \frac{p}{16\pi^2 c} \left\{ 4p \int_0^b x (\ln x)^2 e^{-x^2+2x\sqrt{p}} dx - 8p \ln b \int_0^b x \ln x e^{-x^2+2x\sqrt{p}} dx + 4p (\ln b)^2 \int_0^b x e^{-x^2+2x\sqrt{p}} dx \right. \\
& - 8\sqrt{p} \int_0^b x^2 (\ln x)^2 e^{-x^2+2x\sqrt{p}} dx + 16\sqrt{p} \ln b \int_0^b x^2 \ln x e^{-x^2+2x\sqrt{p}} dx - 8\sqrt{p} (\ln b)^2 \int_0^b x^2 e^{-x^2+2x\sqrt{p}} dx \\
& \left. + 4 \int_0^b x^3 (\ln x)^2 e^{-x^2+2x\sqrt{p}} dx - 8 \ln b \int_0^b x^3 \ln x e^{-x^2+2x\sqrt{p}} dx + 4 (\ln b)^2 \int_0^b x^3 e^{-x^2+2x\sqrt{p}} dx \right\} \quad (3.2.1.6)
\end{aligned}$$

the following serial expansion formula for the term $e^{2x\sqrt{p}}$ in Eq.(3.2.1.6) are used (Gradshteyn and Ryzhik, 1965):

$$e^{\pm x} = \sum_{i=0}^{\infty} (\pm 1)^i \frac{x^i}{i!} \quad (3.2.1.7)$$

A dimensionless value of $B^{*1}(T)$ in Eq.(3.2.1.6) can be obtained as:

$$\begin{aligned}
B^{*1}(T) = & \frac{p}{16\pi^2 c} \{C(p, b) + D(p, b) + E(p, b) + F(p, b) + G(p, b) + H(p, b) + K(p, b) + \\
& L(p, b) + M(p, b)\} \quad (3.2.1.8)
\end{aligned}$$

where the analytical solutions of nine integrals appearing in Eq.(3.2.1.6) are given in the same order in Eq.(3.2.1.8) and expressions $C(p, b)$, $D(p, b)$, $E(p, b)$, $F(p, b)$, $G(p, b)$, $H(p, b)$, $K(p, b)$, $L(p, b)$ and $M(p, b)$ are defined as, respectively.

$$C(p, b) = 4p \sum_{i=0}^n \frac{N(i, b)}{i!} (2\sqrt{p})^i \quad (3.2.1.9)$$

$$D(p, b) = -8p \ln b \sum_{i=0}^n \frac{S(i, b)}{i!} (2\sqrt{p})^i \quad (3.2.1.10)$$

$$E(p, b) = 2p(\ln b)^2 (1 - e^{-b(b-2\sqrt{p})}) + e^p \sqrt{p} \sqrt{\pi} (Erf(b - \sqrt{p}) + Erf(\sqrt{p})) \quad (3.2.1.11)$$

$$F(p, b) = -8\sqrt{p} \sum_{i=0}^n \frac{N(i+1, b)}{i!} (2\sqrt{p})^i \quad (3.2.1.12)$$

$$G(p, b) = 16\sqrt{p} \ln b \sum_{i=0}^n \frac{S(i+1, b)}{i!} (2\sqrt{p})^i \quad (3.2.1.13)$$

$$H(p, b) = -2\sqrt{p}(\ln b)^2 e^{-b^2} (-2e^{2b\sqrt{p}}(b + \sqrt{p}) + 2e^{b^2}\sqrt{p} + e^{b^2+p}(1 + 2p))\sqrt{\pi}(\text{Erf}(b - \sqrt{p}) + \text{Erf}(\sqrt{p})) \quad (3.2.1.14)$$

$$K(p, b) = 4 \sum_{i=0}^n \frac{N(i+2, b)}{i!} (2\sqrt{p})^i \quad (3.2.1.15)$$

$$L(p, b) = -8 \ln b \sum_{i=0}^n \frac{S(i+2, b)}{i!} (2\sqrt{p})^i \quad (3.2.1.16)$$

$$M(p, b) = (\ln b)^2 e^{-b^2} (2e^{b^2}(1 + p) - 2e^{2b\sqrt{p}}(1 + b^2 + b\sqrt{p} + p) + e^{b^2+p}\sqrt{p}(3 + 2p))\sqrt{\pi}(\text{Erf}(b - \sqrt{p}) + \text{Erf}(\sqrt{p})) \quad (3.2.1.17)$$

The general functions N and S appearing in Eqs.(3.2.1.9), (3.2.1.10), (3.2.1.12), (3.2.1.13), (3.2.1.15), (3.2.1.16) can be defined as:

$$\begin{aligned} N(n, b) = & \frac{1}{8} \left(4\Gamma\left(\frac{n}{2} + 1\right) (\ln b)^2 - 4\Gamma\left(\frac{n}{2} + 1, b^2\right) (\ln b)^2 - 4\Gamma\left(\frac{n}{2} + 1\right) \ln b \ln b^2 + \right. \\ & \Gamma\left(\frac{n}{2} + 1\right) (\ln b^2)^2 - 4 \ln b G_{2,3}^{3,0} \left(b^2 \left| \begin{matrix} 1 \\ 0 \end{matrix} \right. \begin{matrix} 1 \\ 0 \\ \frac{n+2}{2} \end{matrix} \right) - 2 G_{3,4}^{4,0} \left(\begin{matrix} 1 & 1 & 1 \\ 0 & 0 & 0 \end{matrix} \left| \begin{matrix} 1 \\ 0 \\ \frac{n+2}{2} \end{matrix} \right) + \right. \\ & \left. 2\Gamma\left(\frac{n}{2} + 1\right) (2 \ln b - \ln b^2) \psi^0\left(\frac{n}{2} + 1\right) + \Gamma\left(\frac{n}{2} + 1\right) \left(\psi^0\left(\frac{n}{2} + 1\right)\right)^2 + \Gamma\left(\frac{n}{2} + 1\right) \psi^1\left(\frac{n}{2} + 1\right) \right) \end{aligned} \quad (3.2.1.18)$$

$$\begin{aligned} S(n, b) = & -\frac{1}{4} \left(2\Gamma\left(\frac{n}{2} + 1, b^2\right) \ln b + G_{2,3}^{3,0} \left(b^2 \left| \begin{matrix} 1 \\ 0 \end{matrix} \right. \begin{matrix} 1 \\ 0 \\ \frac{n+2}{2} \end{matrix} \right) + \Gamma\left(\frac{n}{2} + 1\right) (-2 \ln b + \ln b^2 - \right. \\ & \left. \psi^0\left(\frac{n}{2} + 1\right)) \right) \end{aligned} \quad (3.2.1.19)$$

Gamma, incomplete gamma, polygamma and Meijer G functions in Eqs.(3.2.1.18) and (3.2.1.19) can be given as, respectively (Gradshteyn and Ryzhik, 1965; Copuroglu and Mehmetoğlu, 2015; Mamedov and Copuroglu, 2016; Copuroglu, 2017).

$$\Gamma(s) = \int_0^{\infty} t^{s-1} e^{-t} dt \quad (3.2.1.20)$$

$$\Gamma(s, x) = \int_x^{\infty} t^{s-1} e^{-t} dt \quad (3.2.1.21)$$

$$\psi^n(z) = \frac{d^n \Gamma'(z)}{dz^n \Gamma(z)} \quad (3.2.1.22)$$

$$G_{p,q}^{m,n} \left(z \left| \begin{matrix} a_1, \dots, a_p \\ b_1, \dots, b_q \end{matrix} \right. \right) = \frac{1}{2\pi i} \int_{\gamma L} \frac{\prod_{j=1}^m \Gamma(b_j - s) \prod_{j=1}^n \Gamma(1 - a_j + s)}{\prod_{j=m+1}^q \Gamma(1 - b_j + s) \prod_{j=n+1}^p \Gamma(a_j - s)} z^s ds \quad (3.2.1.23)$$

3.2.2. Computational results of quantum correction to the SVC and its applications on some atoms and molecules

In Table 3.6, all necessary parameters for each atom and molecule are provided in order to calculate Eqs. (3.2.1.6) and (3.2.1.8). By using these values from Table 3.6., the first quantum correction to SVC with Morse potential analytical calculation results for the gases of *He, Ne, Ar, Kr, Xe, CH₄, CO₂* and *N₂* are displayed in Table 3.7. for the temperatures down to boiling points of each specific gas except for the lighter atoms such as *He* and *Ne*. The boiling points temperature limits are chosen since the virial expansion diverges at a specific densities and temperatures (not quite appropriate for liquids) but lighter atoms are exceptional since classical statistics approach of virial expansions is not valid anymore for boiling point of *He* gas (4.222 °K) and *He* data is suggested not to be considered below 40 °K (McQuarrie, 1976).

The comparative results between the quantum correction to SVC with Morse and Lennard-Jones (12-6) potentials displayed in Table 3.7. indicate two important facts depending on temperature and type of the atoms and molecules. In Table 3.7., the dimensionless quantum corrections of SVC with Morse $B^{*1}(T)_M$ and Lennard- Jones (12-6) $B^{*1}(T)_{L-J}$ represent the same pattern for each molecule having very close quantum correction results for high temperatures but quantum correction with Morse potential results gradually become more significant with decreasing temperature that might be due to stronger attractive interaction structure of the Morse potential (McCarty and Babu, 1970). This heavy quantum correction with Morse potential at low temperature effect is more notable for lighter molecules and gradually decreases for heavier molecules as seen from Table 3.7. total quantum correction to SVC with Morse potential results $\Lambda^{*2} b_0 B^{*1}(T)$.

The last two columns of Table 3.7. represent the analytical evaluation of classical SVC with Morse potential $B^0(T)_M$ and Lennard-Jones potential $B^0(T)_{L-J}$ results for corresponding temperatures in order to determine the quantum contribution effects on the classical SVC with two different potentials. Noting that, the negative signs appearing before the classical terms indicate a dominant attractive intermolecular interactions, but quantum correction terms are always positive (Mcquarrie, 1976).

The results of this work conclude that potentials showing more attractive interactions than Lennard-Jones (12-6) such as Morse and Stockmayer might have important contributions of quantum correction to SVC for relatively heavier atoms and molecules. The similar results from literature using Stockmayer potential for quantum correction to SVC confirm this statement (McCarty and Babu, 1970). Therefore, results of this work may help improve the accuracy of thermodynamic properties of the heavier atoms and molecules at low temperatures, providing accurate analytical data to include quantum effects.

Table 3.6. Morse, Lennard- Jones and quantum mechanical parameters used for calculations in Table 3.7.

	Morse Paramaters (Matsumoto, 1987)			Lennard- Jones parameters (Matsumoto, 1987; Mamedov and Somuncu, 2014)		Quantum mechanical parameter (Hirschfelder et al., 1954)
	D/k_B (°K)	r_e (Å)	α (Å ⁻¹)	D/k_B (°K)	σ (Å)	Λ^*
He	12.6	2.92	2.197	10.22	2.56	2.67
Ne	51.3	3.09	2.036	35.6	2.75	0.593
Ar	118.1	4.13	1.253	120	3.40	0.186
Kr	149.0	4.49	1.105	171	3.60	0.102
Xe	226.9	4.73	1.099	220	4.10	0.064
CH₄	149.1	4.50	1.166	148.4	3.81	0.239
CO₂	196.7	5.18	1.02	189	4.48	0.0804
N₂	93.4	4.43	1.166	95.9	3.706	0.228

Table 3.7. The comparative calculation results of quantum correction to SVC with Morse and Lennard-Jones (12-6) potentials.

	$T(K)$	$\Lambda^{*2}b_0B^{*1}(T)_M$ (cm^3/mol)	$\Lambda^{*2}B^{*1}(T)_M$	$B^{*1}(T)_M$ Eq.(3.2.1.8)	$B^{*1}(T)_{L-J}$ (Somuncu et al., 2019)	$B^0(T)_M$ (cm^3/mol) (Matsumoto, 1987)	$B^0(T)_{L-J}$ (cm^3/mol) Mamedov and Somuncu, 2014)
He	256	0.620983	0.0293461	0.0041165	0.00301586	11.9165	11.1838
	163.8	1.17205	0.0553883	0.00776955	0.0051656	12.0519	10.903
	83.5	3.28254	0.155125	0.02176	0.0121032	10.7904	8.85924
	64	5.27642	0.249351	0.0349774	0.0172638	9.48849	7.17024
	40.9	12.5087	0.591129	0.0829201	0.0325495	5.55298	2.44914
Ne	890	0.0455055	0.00173483	0.0049334	0.00302287	13.8922	13.8633
	557	0.0899740	0.00343012	0.00975438	0.00532031	13.7478	13.4734
	392	0.154335	0.0058838	0.0167320	0.00824122	12.9234	12.4978
	222.5	0.418476	0.0159537	0.0453684	0.0173099	9.4141	8.86959
	142.4	1.05224	0.0401152	0.114077	0.0325731	3.38414	3.02745
	95	3.06185	0.116728	0.331945	0.0610677	-6.653	-6.20557
	57	18.2717	0.696581	1.9809	0.151338	-31.8123	-27.5516
Ar	900	0.0253301	0.000510964	0.0147695	0.0135492	19.7215	19.6465
	700	0.0386980	0.000780624	0.0225640	0.0190251	15.8243	15.4605
	500	0.0707185	0.00142655	0.0412345	0.0306725	7.46732	7.02514
	300	0.199967	0.00403378	0.116597	0.0680158	-16.1271	-15.4972
	200	0.537735	0.0108473	0.313542	0.140083	-51.3545	-47.8059
	100	5.7881	0.116759	3.37492	0.654731	-193.948	-172.516
	87.29	10.6843	0.215527	6.22983	0.945785	-247.965	-218.326
Kr	900	0.0131783	0.000223939	0.0215243	0.0219473	17.028	15.7565
	700	0.0206311	0.000350595	0.0336981	0.0314805	9.23382	7.67843
	500	0.0392666	0.000667277	0.0641365	0.0526836	-6.8245	-8.25538
	300	0.123126	0.00209234	0.201109	0.127118	-51.2354	-50.6705
	200	0.37938	0.006447	0.619665	0.290023	-118.094	-113.178
	120.85	2.50218	0.0425207	4.08696	1.02619	-289.508	-272.564
Xe	900	0.0158788	0.000182666	0.0445962	0.0315107	8.55413	11.3064
	700	0.0261108	0.000300371	0.0733329	0.0461072	-7.03685	-5.28859
	500	0.0547254	0.000629547	0.153698	0.0799171	-38.587	-37.8982
	300	0.218996	0.00251927	0.615057	0.208791	-127.101	-125.808
	200	0.964258	0.0110926	2.70815	0.524327	-268.851	-260.319
	166.1	2.21043	0.0254282	6.20805	0.852911	-376.286	-358.843
CH₄	900	0.0858647	0.00123092	0.0215494	0.0180359	22.1221	22.8098
	700	0.134029	0.00192138	0.033637	0.0256296	14.9504	14.8925
	500	0.254273	0.00364516	0.0638147	0.0421936	0.0616688	-0.818914
	300	0.784843	0.0112512	0.196971	0.098092	-41.3699	-42.5704
	200	2.40897	0.034534	0.604576	0.213946	-103.98	-103.242
	111.65	22.8895	0.328134	5.74455	0.861177	-306.099	-289.714
CO₂	900	0.0254415	0.000224152	0.0346993	0.0252848	22.4848	24.8008
	700	0.0409242	0.000360562	0.0558158	0.0365358	6.15843	7.02238
	500	0.0823397	0.000725454	0.112302	0.0619412	-27.058	-27.957
	300	0.296164	0.00260935	0.403933	0.153911	-119.59	-121.399
	194.65	1.25768	0.0110808	1.71533	0.387611	-277.574	-273.612
N₂	900	0.0330619	0.000514936	0.00992174	0.0101081	27.0828	28.8338
	700	0.0496851	0.00077384	0.0149103	0.0140464	23.9397	24.9508
	500	0.0882299	0.00137417	0.0264774	0.0222395	16.7783	16.9116
	300	0.232046	0.0036141	0.0696361	0.0473478	-4.17354	-4.88676

	200	0.565899	0.00881382	0.169824	0.0928184	-35.5581	-36.0363
	100	4.34164	0.0676206	1.30291	0.376509	-157.307	-151.446
	77.355	12.1711	0.189563	3.65248	0.713356	-249.88	-236.369

4. CONCLUSION

The Virial Equation of State considers molecular sizes and attractive –repulsive forces between atoms and molecules via intermolecular potential, which is essential for describing the behavior of real gases. The SVC representing the first deviation from the ideal gas has numerous applications including gases, liquids, neutral parts of partially ionized plasmas, fully ionized plasmas under constant magnetic field, quantum SVC calculations and osmotic SVC for biological purposes. One of the most important effects of determining the value of SVC is the choice of intermolecular potential which is the Morse potential for this study since its features are proper for the evaluation of the SVC at high temperature range. The analytical evaluation of SVC using Morse potential might be an appropriate choice for the plasma and high temperature gas studies since the repulsive forces, represented by an exponential term within the Morse potential, are more effective at high temperature region.

The analytical formula in Eq.(3.1.1.10) is established by using binomial expansion theorem, exponential series expansion formula and some special functions in Mathematica 10 software. The real system applications of the obtained analytical formula of SVC with Morse potential are demonstrated on neutral atom gases and plasmas of *B, Si, Zn, H₂, N₂, O₂, NO, CO, He, Ne, Ar, Kr, Xe* and provided reliable and accurate data since our study doesn't have any parameter restrictions. An approximate maximum temperature is specifically chosen for every atom and molecule considering its specific ionization energy to make sure the gas still includes neutrals. Similarly, a minimum specific temperature is considered for every substance to avoid temperatures below the liquid phase transition.

The results of obtained analytical formula for the SVC with Morse potential in Eq.(3.1.1.10) are compared with both numerical and another analytical formula from literature (Matsumoto, 1987). Tables 3.2-3.4 includes these comparative results of SVC with Morse potential for *, Si, Zn, H₂, N₂, O₂, NO, CO, He, Ne, Ar, Kr, Xe* gases at different temperatures and Figures 3.1-3.3 illustrates the results of Eq.(3.1.1.10). The negative signs of SVC results in Table 3.3 indicate the existence of dominant attractive intermolecular forces between gas

molecules and the positive signs in Table 3.2 and Table 3.4 denote repulsive intermolecular forces at corresponding temperatures. The main obstacle of the compared literature is its approximation of $b \rightarrow \infty$ in Eq.(3.1.1.7), which loses its validity at high temperature region with a gas of lower values of Morse parameters ($b = \sqrt{\frac{D}{k_B T}} e^{\alpha r_e} \rightarrow 0$). It can be deduced that, our analytical formula for the evaluation of the SVC has advantages over the literature especially at high temperatures since it does not include any approximations. Therefore, our analytical formula is valid for all values of parameters, creating accurate thermodynamic properties such as speed of sound.

The thermodynamic properties of substances can be calculated by using obtained analytical formula of SVC with Morse potential by using Eq.(2.5.6) and Eq.(3.1.1.4). As a real system application, the speed of sound of N_2 , Ar and Zn gases are calculated and tabulated for temperatures between 3000-7000 °K for 0.1 and 1 atm pressures in Table 3.5. The higher pressure speed of sound results displayed more deviations from the ideal speed of sound values except for Zn at 3000-6000 °K. This unexpected behavior of Zn might be due to the negative signs of SVC values at 3000-6000 °K which represent attractive forces and form a reduced pressure effect inside the gas. The remaining results are compared with literature data from NASA and found to produce satisfying data.

The virial EoS diverges at low temperature region nearby gas-liquid transition due to quantum effects at high density and low temperatures, which can be corrected by the quantum correction terms. The first quantum correction using the Morse potential has been evaluated analytically and applied to He , Ne , Ar , Kr , Xe , CH_4 , CO_2 and N_2 gases for the low temperature range nearby liquid transition region which density of every gas increases significantly. Since lighter atoms are more vulnerable to quantum effects, He data for quantum correction is not provided for below 40 °K as recommended in literature (McQuarrie, 1976). In a study (Bruch, 1967), first quantum correction to SVC is evaluated with an approximation limiting its real system application on gases, but our study provides exact analytical solution without any parameter restrictions using binomial expansion, exponential series expansion and special functions in Mathematica 10 software.

Table 3.6. includes first quantum correction to SVC results for Morse and Lennard-Jones (6-12) potentials for the comparison. The classical SVC results of Morse and Lennard-Jones (6-

12) potentials are also included in Table 3.7 since Eq.(3.2.1.1) expresses that classical and quantum correction of SVC must be added to form total SVC value at a given temperature of a gas. Table 3.7 also demonstrates that although the SVC results may be positive or negative, the first quantum correction results are always positive (McQuarrie, 1976). Table 3.7 displays a similar temperature dependence of first quantum correction values of both Morse and Lennard-Jones (6-12) potentials since temperature reduction creates more quantum effects inside the gas. The analytical calculation results of first quantum correction to SVC with Morse potential compared to literature with corresponding correction data using Lennard-Jones (6-12) potential and found to provide mostly higher correction values than Lennard-Jones (6-12) used results. However, the differences between the results are found to be not significant at higher values of temperature range.

The results of analytical evaluation of SVC and speed of sound using Morse potential is published in Contribution to Plasma Physics (Mamedov and Cacan, 2019). Besides, the findings of analytical evaluation of first quantum correction to SVC using Morse potential is published in Journal of Chemical Thermodynamics (Cacan and Mamedov, 2019).

Our next goal is to achieve a more practical analytical solution for the SVC with Morse potential so that its first and second temperature derivatives can be calculated easily to consider in calculations of thermodynamic properties.

5. REFERENCES

- Al-Maaitah, I. F., 2018, Quantum Second Virial Coefficients for Krypton -86 Gas, *Appl. Phys. Res.* 10, 1.
- Apfelbaum, E. M., 2013, The Electron Transport Coefficients of Boron and Silicon Plasma, *Contr. Plasma Phys.* 53, 317.
- Apfelbaum, E. M., 2016, The Thermophysical Properties of Iron Plasma, *Contr. Plasma Phys.* 56, 176.
- Apfelbaum, E. M., 2017, Calculation of Thermophysical Properties of Titanium and Zinc Plasmas., *High. Temp.*, 55, pp 1-11.
- Apfelbaum, E. M., 2017, The Calculations of Thermophysical Properties of Molybdenum Plasma, *Phys. Plasmas.* 24, 052702.
- Arda, A. and Sever, R., 2011, Bound State Solutions of Schrödinger Equation for Generalized Morse Potential with Position-Dependent Mass, *Commun. Theor. Phys.* 56, 51.
- Aziz, R. A., 1993, A highly accurate interatomic potential for argon, *J. Chem. Phys.*, 99, 4518.
- Baus, M. and Colot, J. L., 1987, Thermodynamics and Structure of a Fluid of Hard Rods, Disks, Spheres, or Hyperspheres from Rescaled Virial Expansions., *Phys. Rev. A* 36, pp-3912-3925.
- Beattie, J. A. and Bridgeman, O., 1928, A New Equation of State for Fluids. *Proc. Am. Acad. Arts and Sci.*, 63, 229-308.
- Beattie, J. A. and Bridgeman, O., 1927, A New Equation of State for Fluids. I. Application to Gaseous Ethyl Ether and Carbon Dioxide. *Journal of American Chemical Society*, 49 (7),1665-1667.
- Boyd, M. E. and Larsen S. Y., 1967, Quantum Mechanical Calculations of the Second Virial Coefficients for Hydrogen., *Natl. Bur. Stand. (U. S.)*, 412.
- Boyd, M. E., 1970, Quantum Corrections to the Second Virial Coefficient for the Lennard-Jones (m-6) Potential, *J. Res. Nat. Bur. Stand.* 75A, 57.
- Bruch, L. W., 1967, Second Virial Coefficient for the Exponential Repulsive Potential, *Phys. Fluids*, 10, 2531.
- Bruch, L. W., 1971, Qualitative Aspects of the Quantum Mechanical Second Virial Coefficient. *J. Chem. Phys.*, 54 (10), 4281-4282.
- Cacan, H. and Mamedov, B. A., 2019, The Comparative Analytical Evaluation of Quantum Corrections to The Second Virial Coefficient with Morse potential and its Applications to Real Systems., *J. Chem. Thermodyn.*, 138,147-150.
- Calvert, J. B. and Amme, R. C., 1966, Three-Dimensional Morse-Potential Calculation of Vibrational Energy Transfer: Application to Diatomic Molecules, *J. Chem. Phys.* 45, 4710.
- CEARUN, NASA, <https://cearun.grc.nasa.gov> [retrieved 2018].
- Copuroglu, E. and Mehmetoğlu, T., 2015, Full Analytical Evaluation of the Einstein Relation for Disordered Semiconductors, *IEEE Trans. Electron Devices* ,62 , 1580.

- Copuroglu, E., 2017, Evaluation of Self-Friction Three-Center Nuclear Attraction Integrals with Integer and Noninteger Principal Quantum Numbers n over Slater Type Orbitals, 1598951.
- Corbin, N., Meath, W. J. and Allnatt, A. R., 1984, Second Virial Coefficients, Including Quantum Corrections, for Nitrogen Using Model Potentials, *Mol. Phys.*, 53, 225.
- Cristancho, D. E., Acosta-Perez, P. L., Mantilla, I. D., Holste, J. C., Hall, K. R. and Iglesias-Silva, G. A., 2015, A Method To Determine Virial Coefficients from Experimental (p, ρ ,T) Measurements. *J. Chem. Eng. Data*, 60 (12), pp 3682-3687.
- Deming, W.E. and Shupe, L. E., 1931, Some Physical Properties of Compressed Gases. II, Carbon Monoxide, *Phys. Rev.* 38, 2245.
- Dewi, B. P. C., Linden, E., Bot, A. and Venema, P., 2020. Second Order Virial Coefficients from Phase Diagrams. *Food Hydrocolloids*, 101, 105546, pp 1-16.
- Ebeling, W., Fortov, V. E. and Filinov. V., 2017, *Quantum Statistics of Dense Gases and Nonideal Plasmas*, Springer, Switzerland.
- Ebeling, W., Steinberg, M. and Ortner, J., 2000, Ionization Equilibrium and EOS of a Low-Temperature Hydrogen Plasma in Weak Magnetic Fields, *Eur. Phys. J. D.* 12, 513.
- El Kinani, R., Kaidi, H., and Benhamou, M., 2018, Investigation of DNA denaturation from generalized Morse potential, *Materials and Devices*, 3 (2), pp.0207.
- Eliezer, S., Ghatak. A. and Hora, H., *Fundamentals of Equations of State*, World Scientific Publishing Co. Pte. Ltd, 8 p, Singapore.
- Eslami, H., Mozaffari, F. and Baushehri, A., 2001, Calculation of the second virial coefficient of nonspherical molecules: Revisited, *Int. J. Therm. Sci.*, 40, 999-1010.
- Galicia-Pimentel, U.F., Osorio-González, D. and López-Lemus, J., 2006, On the Morse Potential in Liquid Phase and at Liquid-Vapor Interface. *Rev. Mex. Fis.*, 52 (5), 422–428.
- Girifalco, L. A. and Weizer, V. G., 1958, Application of the Morse Potential Function to Cubic Metals. *Phys. Rev.*, 114 (3), pp 687-690.
- Gradshteyn, I. S. and Ryzhik, I. M., 1965, *Table of Integrals, Series and Products*, Academic Press, London.
- Heyes, D. M. and Pereira de Vasconcelos, T., 2017, The Second Virial Coefficient of Bounded Mie Potentials, *J. Chem. Phys.* 147, 214504.
- Hirschfelder, J.O., Curtis, C.F. and Bird, R.B., 1954, *Molecular Theory of Gases and Liquids*, John Wiley & Sons, New York.
- Hou, Y., Czejdo, A. J., DeChant, J., Shill, C. R. and Drut, J. E., 2019. Leading- and next-to-leading-order semiclassical approximation to the first seven virial coefficients of spin-1/2 fermions across spatial dimensions. *Phys. Rev. A* 100, 063627.
- Hryniewicki, M.K., 2011, *Accurate and Efficient Evaluation of the Second Virial Coefficient Using Practical Intermolecular Potentials for Gases*, Ph.D. Thesis, University of Toronto, Toronto, ON, Canada.
- Hussein, N. A., Eisa, D. A. and Eldin, M. G., 2012. The quantum equations of state of plasma under the influence of a weak magnetic field. *Phys. Plasmas*, 19, 052701.
- Johnson, W. R., Guet, C. and Bertsch, G. F., 2006, Optical Properties of Plasmas Based on An Average-Atom Model, *J. Quant. Spectrosc. Radiat. Transfer.* 99, 327.

- Kallmann, H. K., 1950, Thermodynamic Properties of Real Gases for Use in High Pressure Problems, Rand Corp. RM-442, CA.
- Kaplan, I. G., 2006, Intermolecular Interactions: Physical Picture. Computational Methods and Model Potentials. John Wiley & Sons, Inc.
- Karaoğlu, B., 2009, İstatistik Mekanik Giriş, Seçkin Yayıncılık, Ankara.
- Khomkin A. L., and Shumikhin, A.S., 2014, Equation of State, Composition, and Conductivity of Dense Metal-Vapor Plasma, High. Temp. 52, 328.
- Kirkwood, J. G., 1933, Quantum Statistics of Almost Classical Assemblies, Phys. Rev. 44, p. 31.
- Konowalow, D. D., Taylor, M. H. and Hirschfelder, J. O., 1961, Second Virial Coefficient for the Morse Potential, Phys. Fluids. 4, 622.
- Kunz, R. G. and Kapner, R. S., 1969, Second Virial Coefficients from Tabulated P-V-T Data. Results for Chlorotrifluoromethane, Dichlorodifluoromethane, Fluorotrichloromethane, and Trimethyl Borate.
- Landau, L. D. and Lifshitz, E. M., 1980, Statistical Physics, Pergamon Press Ltd.
- Li, L., Pabit, S. A., Lamb, J. S., Park, H. Y. and Pollack, L., 2008, Closing lid on DNA end-to-end stacking interactions, Applied Physics Letters, 92, 223901, pp 1-3.
- Lim, T. C., 2003, The relationship between Lennard-Jones (12-6) and Morse potential functions. Z. Naturforsch. A., 58 (11), 615-617.
- Logan, E., 1999, Thermodynamics: Processes and Applications, 3 p, Marcel Dekker, Inc., New York.
- Lucas, K., 1991, Applied Statistical Thermodynamics, Springer-Verlag Berlin Heidelberg.
- Mamedov B.A. and Somuncu, E., 2014, Analytical Treatment of Second Virial Coefficient over Lennard-Jones (2n – N) Potential and Its Application to Molecular Systems, J. Mol. Struct. 1068, 164.
- Mamedov, B. A. and Cacan, H., 2019, A General Analytical Method for Evaluation of the Thermodynamic Properties of Matters Using Virial Coefficients with Morse Potential at High Temperature, Contrib. Plasm. Phys., 59 (9), pp 1-12.
- Mamedov, B. A. and Copuroglu, E., 2016, Unified Analytical Treatments of The Two-Parameter Fermi Functions Using Binomial Expansion Theorem and Incomplete Gamma Functions, Solid State Commun., 245, 42.
- Mamedov, B. A. and Somuncu, E., 2016, Evaluation of Quantum Corrections to Second Virial Coefficient with Lennard-Jones (12-6) Potential, J. Phys., 766,1, 012010.
- Matsumoto, A., 1987, Parameters of the Morse Potential from Second Virial Coefficients of Gases, Z. Naturforsch, 42 a, 447.
- Mayer J. E. and Careri, G., 1952, Equation of State Computations, J. Chem. Phys. 20, 1001.
- McCarty, M. and Babu, S. V. K., 1970, First Quantum Corrections to The Second Virial Coefficient of A Stockmayer Gas, J. Phys. Chem., 74, 5, 1113.
- McQuarrie, D. A., 1973, Statistical Thermodynamics, University Science Books, CA, 116 p.
- McQuarrie, D.A., 1976, Statistical Mechanics. Harper & Row, New York, 224-227.
- Methods and Model Potentials. John Wiley & Sons, America, 141-146.
- Monajjemi, M., Naderi, F., Mollaamin F., and Khaleghian, M., 2012, Drug Design Outlook by Calculation of Second Virial Coefficient as a Nano Study. J. Mex. Chem. Soc. 56 (2), pp.207-211.

- Naderi, F., Yari, M., Mollaamin, F., Ilkhani, A. R., Khaleghian, M., Monajjemi, M. and Khodayari, N., 2009, A New Modification of Morse Potential Energy Function. *J. Phys. Theor. Chem.*, 5 (4), 183-187.
- Olla, P., 2015. *An Introduction to Thermodynamics and Statistical Physics*, Switzerland: 5 p, Springer.
- Omarbakiyeva, Y., (Doctoral dissertation), Cluster Virial Expansion for the Equation of State of Partially Ionized Hydrogen Plasma. University of Rostock, Germany (2010).
- Pateyron, B., Elchinger, M.-F., Delluc, G. and Fauchais P., 1992. Thermodynamic and Transport Properties of Ar-H₂ and Ar-He Plasma Gases Used for Spraying at Atmospheric Pressure. I: Properties of the Mixtures. *Plasma Chem. Plasma P.*, 12 (4), 421-447.
- Peng, D. Y. and Robinson, D. B., 1976. A New Two-Constant Equation of State. *Industrial Engineering Chemistry Fundamentals*, 15 (1), 59-64.
- Pitzer, K. S. and Curl, R. F., The Volumetric and Thermodynamic Properties of Fluids. III. Empirical Equation for the Second Virial Coefficient., *Journal of American Chemical Society*, 79, 2369.
- Recoules, V., Lambert, F., Decoster, A., Canaud, B. and Cle'rouin, J., 2009, Ab Initio Determination of Thermal Conductivity of Dense Hydrogen Plasmas, *Phys. Rev. Lett.* 102, 075002.
- Rydberg, V. R., 1931, *Graphische Darstellung Einiger bandenspektroskopischer Ergebnisse*, Physikalisches Institut der Hochschule, Stockholm.
- Saxena, S. C., and Gambhir, R. S., 1963, Second Virial Coefficient of Gases and Gaseous Mixtures on The Morse Potential, *Mol. Phys.* 6, 577.
- Schultz, A. J. and Kofke, D. A., 2014. Fifth to eleventh virial coefficients of hard spheres. *Phys. Rev. E*, 90, 023301-14.
- Sinanoğlu, O. and Pitzer, K. S., 1959, Equilibrium Properties of Hydrogen Gas from 5000° to 20 000°K, *J. Chem. Phys.* 31, 960.
- Somuncu E., 2014, 'Calculation of Second and Third Virial Coefficients for Different Potentials and Application of some of the Molecules.', PhD thesis, Gaziosmanpasa University, 2 p, Tokat.
- Somuncu, E., 2018, Accurate Assessment of the Boyle Temperature of Nonpolar Molecular Gases Using Second Virial Coefficient with Lennard-Jones (12-6) Potential, *Indian J Phys*, 93 (5).
- Somuncu, E., Oner, F., Orbay, M. and Mamedov B. A., 2019, A comparative evaluation of speed of sound and specific heat capacities of gases by using the quantum mechanical and classical second virial coefficients. *J Math Chem* 57, 1935–1948.
- Song, Y. and Mason, E. A., 1990. Analytical Equation of State for Molecular Fluids: Comparison with Experimental Data., 42 (8) pp 4749-4755.
- Steinberg, M., Ebeling, W and Ortner, J., 2000. Second virial coefficient for the Landau diamagnetism of a two-component plasma. *Phys. Rev. E*, 61, 2290.
- Ushcats, M.V., Ushcats, S.J. and. Mochalov, A.A., 2016. Virial Coefficients of Morse Potential., *Ukr. J. Phys.*, 61 (2), 160-167.
- Van, T. P., 2006, 'Ab initio calculation of intermolecular potentials, prediction of second virial coefficients for dimers H₂-H₂, H₂-O₂, F₂-F₂ and H₂-F₂, and Monte Carlo

- simulations of the vapor-liquid equilibria for hydrogen and fluorine', PhD thesis, University of Cologne, 2 p Köln.
- Vargas, P., Muñoz, E. and Rodriguez, L., 2001, Second Virial Coefficient for the Lennard–Jones Potential, *Physica A*. 290, 92.
- Varshni, Y. P., 1957. Comparative Study of Potential Energy Functions for Diatomic Molecules., *Reviews of Modern Physics*, 29 (4), pp 664-682.
- Wilson, W. W. and DeLucas, L. J., 2014. Application of the Second Virial Coefficient: Protein Crystallization and Solubility, *Acta Crystallographica*, F70, 543-554.
- Zeng, X. L., Ju, X. H. and Xu, S. Y., 2012. Interatomic Potential and Thermodynamic Property of Diatomic Uranium, *Adv. Mat. Res.*, 550, p 2810.
- Zhen, S. and Davies, G. J., 1983. Calculation of the Lennard- Jones $n - m$ Potential Energy Parameters for Metals. *Phys. Stat. Sol. (a)* 78, pp 595-605.



6. RESUME

Hatun aan was born in Berlin. She received her Bachelor's degree from Department of Physics, Atatürk University, Erzurum in 2005. After graduation, she was accepted to Department of Physics at Karadeniz Technical University for her direct doctoral degree and studied English at School of Foreign Languages at Karadeniz Technical University in 2006. She also received scholarship from the Scientific and Technological Research Council of Turkey in 2007. She earned a scholarship from Ministry of Education for her language education and master's degree abroad in 2007. She completed her master's degree at department of Physics and Astronomy, Georgia State University at U.S.A in 2011.

